



# **Design of a Ku-band Instrumentation Synthetic Aperture Radar System**

---

A Major Qualifying Project  
submitted to the Faculty of the  
WORCESTER POLYTECHNIC INSTITUTE  
in partial fulfillment of the requirements for the  
Degree of Bachelor of Science

By

David Kelly

Date: 14 October 2015

MIT Lincoln Laboratory Supervisor: Andrew Messier

Approved:

---

**Professor Donald R. Brown, Major Advisor**

This work is sponsored by the Department of the Air Force under Air Force Contract #FA8721-05-C-0002. Opinions, interpretations, recommendations and conclusions are those of the authors and are not necessarily endorsed by the United States Government.

Approved for public release.

## Table of Contents

1. Abstract.....	4
2. Introduction .....	5
3. Background .....	6
3.1 Conventional Radars .....	6
3.2. Synthetic Aperture Radars .....	8
3.3. Stretch Processing.....	10
3.4. Bistatic Radars Testing .....	12
4. Methodology.....	13
4.1. Creating a Ku-band SAR System.....	13
4.1.1 Selecting Initial Components .....	13
4.1.2. Component Testing.....	15
4.1.3. Waveform Lab Testing and Measurements.....	16
4.2. Radar Model Design.....	17
4.3. Field Testing, Data Collection, and Analysis.....	17
4.3.1. Stationary Corner Reflector Test .....	18
4.3.2. Moving Corner Reflector Test.....	18
4.3.3. Analyzing the Test Data .....	20
5. System Design .....	21
5.1. Final Components .....	21
5.1.1. Output from the Reference Oscillator .....	22
5.1.2. Waveform Alteration .....	22
5.1.3. AWG to M20220HA Mixer .....	23
5.1.4. From M20220HA through Transmission.....	24
5.1.5. Receiving Path of the Radar System .....	25
5.2. AC to DC Converters.....	26
5.3. Final Design and CAD Model.....	26
5.4. Waveform Selection.....	30
6. Results.....	32
6.1. Lab Measurements .....	32
6.2. Stationary Target.....	34
6.3. Moving Target .....	38

6.4. Calculated Results .....	42
7. Conclusions .....	45
8. Acknowledgements.....	47
9. Bibliography .....	48

## Table of Figures

Figure 1: Antenna aperture.....	7
Figure 2: Synthetic aperture value.....	8
Figure 3: Stretch processing.....	11
Figure 4: Initial design block diagram. ....	14
Figure 5: Stationary targets.....	18
Figure 6: Moving target.....	19
Figure 7: Final radar system model.....	21
Figure 8: Oscillator connections.....	22
Figure 9: Lo and IF ports of the M20220HA mixer.....	24
Figure 10: M20220HA RF port to the HMC-C051 mixer without the PA and LNA.....	25
Figure 11: HMC-C051 mixer to the SDR.....	25
Figure 12: System model.....	27
Figure 13: CAD model. ....	28
Figure 14: Final radar system design. ....	29
Figure 15: Lower level of the radar design. ....	29
Figure 16: PA and LNA housing. ....	30
Figure 17: Useable bandwidth. ....	33
Figure 18: Interference from two generators from Christopher Panuski’s presentation on LiTE SAR ground data collection. ....	33
Figure 19: Range sidelobe power levels. ....	34
Figure 20: Parking garage test map. ....	35
Figure 21: Far data point.....	36
Figure 22: Close data point. ....	36
Figure 23: Data from Christopher Panuski’s presentation on LiTE SAR ground data collection. ....	38
Figure 24: Ranged-Doppler graph.....	39
Figure 25: Ranged-Doppler compared to range profile.....	39
Figure 26: Extra targets in the scene. ....	40
Figure 27: Intermodulation products removed. ....	41
Figure 28: Updated ranged profile.....	42
Figure 29: SAR sensitivity values.....	43
Figure 30: High dynamic range data set. ....	46
Figure 31: Spectrogram of output signal. ....	46

## Table of Tables

Table 1: Variables for Equations .....	6
Table 2: Initial parts list.....	14
Table 3: Initial parts selection. ....	15
Table 4: Voltage and current requirements.....	26
Table 5: Noise equivalent sigma nought parameters. ....	43

## 1. Abstract

This project focused on designing a Ku-band instrumentation SAR system for use by Group 105 at MIT Lincoln Labs. Group 105 had an existing Ku-band SAR system intended for use on unmanned airborne platforms. The small form factor required for use on an airborne platform led to several design decisions that limit the achievable performance of the existing SAR. This project focused on developing a new instrumentation-grade SAR with better performance than the existing SAR and not subject to the small form factor constraints of the existing SAR. The new instrumentation-grade SAR is based on readily-available parts. The new SAR system was thoroughly tested in the laboratory space to verify the design and then field tested on top of the MIT Lincoln Labs parking garage. The data collected from the laboratory tests and field tests were compared to the existing radar system and the new radar system was shown to meet or exceed all of the performance objectives of the project.

## 2. Introduction

The Airborne Radar Systems and Techniques Group (Group 105) at MIT Lincoln Laboratory (MIT LL) have developed a small form-factor Ku band Synthetic Aperture Radar (SAR) for use on aerial drones. Group 105 have also been using this radar as an instrumentation radar system to help develop signal processing algorithms, perform phenomenology measurements, and conduct bistatic radar proof of concept tests. Due to the requirement of a small form-factor, performance was sacrificed in the design. This performance trade-off makes it less than ideal as an instrumentation radar system. This Major Qualifying Project will focus on the re-design of the current Ku-band SAR as a chassis-based Ku-band SAR that will be optimized for use as an instrumentation radar.

Some drawbacks of the existing Ku-band SAR were: the use of an analog PLL waveform synthesizer which introduced non-linearity, Radio Frequency (RF) isolation issues, a lack of real-time display functionality, and the requirement of manual data transfer via flash drive. Use of an analog PLL waveform synthesizer introduced non-linearity caused by tracking errors in the PLL's analog loop filter response into the system. This produced undesired frequency content that corrupted the LFM chirp waveform used by the SAR, thus causing measurement error. Since the analog waveform is an approximation of a linear chirp, linearity errors lead to a non-ideal autocorrelation response between the reference waveform and the returned target waveform. In practice the sidelobes that result from the non-ideal response caused blurring in the ideal point response. While the point response was adequate for field use, it needs to be more focused for use as an instrumentation radar system.

In order for the SAR to have a small form-factor, many of the components of the radar were combined into single boards populated with Monolithic Microwave Integrated Circuits (MMIC's). While using MMIC's decreases the overall size of the radar, they can cause electromagnetic field (EMF) interference issues with neighboring components. Close proximity between different boards exacerbated this interference issue such that the isolation between components was poor. This interference issue can lower the signal-to-noise ratio (SNR) and corrupt measurements. If a signal has too much noise, the usable bandwidth of the signal is reduced. The previous radar design could only use about half of the bandwidth allocated to Group 105. Since the new radar will be used to conduct phenomenology measurements, the entire bandwidth allotted to Group 105 should be able to be used for more accurate measurements.

Because the SAR was designed to be attached to an Unmanned Aerial Vehicle (UAV), the data collected by it was stored on a flash drive that had to be removed after each test to collect the data. There was also no way to stream the data. While these issues do not affect the performance of the SAR, it makes it more tedious to use it for testing purposes.

The purpose of this project was to create a new instrumentation radar system for Group 105 that is not limited by the form factor and power requirements of the previous SAR system. The radar system created during this project was tested both in a lab environment as well as on top of the MIT Lincoln Labs parking garage. Data had been collected at the same location using the existing radar system before the start of this project. This allowed for comparisons to be made between the two systems using data collected in the same location in similar circumstances.

### 3. Background

For this project, it is necessary to have a clear understanding of what a synthetic aperture radar system is and how it is used. As the radar to be designed will use stretch processing to determine a target's distance from the radar, knowledge in how stretch processing works is required as well. Group 105 has plans to use this radar to conduct bistatic radar proof of concept tests. It will be helpful to have information on what a bistatic synthetic aperture radar is, how it differs from a normal synthetic aperture radar, and what kind of impact the research and development of bistatic SAR's would have for Department of Defense. Table 1 lists the variables and their corresponding symbols and units used for the equations in this report.

Symbol	Variable	Unit
P	Power	W
G	Antenna Gain	
a	Aperture	m <sup>2</sup>
σ	cross-sectional area	m <sup>2</sup>
S	Detectable signal power	W
d	Distance to target	d
c	Speed of light	m/s
A	Amplitude	m
m	Slope	m/s
t	Time	s
f	Frequency	Hz
B	Bandwidth	Hz
R	Range	m
r	Resolution	m
θ	Angle	radians
K	Boltzman constant = $1.3806488 \times 10^{-23}$	m <sup>2</sup> kg s <sup>-2</sup> K <sup>-1</sup>
T	Temperature	K
N	Noise figure	
L	Loss	dB
τ	Pulse duration	s
λ	Wavelength	m
ρ <sub>a</sub>	3dB length azimuth IRF/ azimuth resolution = $\frac{d\lambda}{L}$ where L = the length of the antenna[1]	m
W <sub>a</sub>	Azimuth Weighting factor (0.886 used in the IEEE Derivation for the case of no weighting)	

Table 1: Variables for Equations

#### 3.1 Conventional Radars

Radio Detection And Ranging (RADAR) systems are used to detect and locate objects by transmitting a specific waveform, and detecting the nature of the echo signal. Unlike cameras or other optical systems, radar systems are not limited by factors such as darkness, fog, rain, etc. Radar systems can also measure the distance away from a target, based off of the time delay of the received signal.

[1] Ulaby, Moore, & Fung. (1986).

Because electromagnetic energy propagates at the speed of light, the time between the sent and received signals is defined as [2 pp.1-2]:

$$t_{\text{echo}}: 2 \frac{d}{c}$$

The range of a radar system is affected by many different factors. A simple model of the maximum range is based on the transmitted power, antenna gain, antenna effective aperture, radar cross section, and minimum detectable signal power. Combining these factors results in the equation [1 p.15]:

$$\text{Max Range: } \sqrt[4]{\frac{P_{tx} G_{rx} \text{effective} \sigma}{(4\pi)^2 S_{min}}}$$

The equation is a simplified calculation of the maximum range of a radar system operating in an environment without any noise factors. Because of this simplification, the true range can be as small as half the calculated value [1 p.15]. This equation does, however show that there is a positive relationship between an antenna's aperture and the max range of the radar system. A depiction of an antenna and its effective aperture is shown in Figure 1. An antenna's aperture is the area of the antenna, perpendicular to an incoming signal, which is receiving the signal.

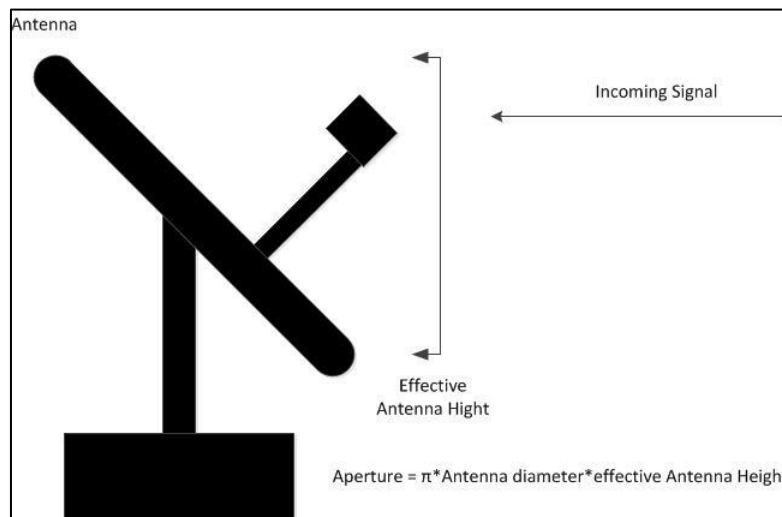


Figure 1: Antenna aperture.

One way conventional radar systems increase their range is to use large antennas. While this method works for stationary radar systems that locate new targets in a known area, it becomes a less ideal solution for radar systems used to map unknown areas, which are often attached to vehicles and need have small form-factors. This project focuses on a radar system that increases the effective

---

[2]Skolnik, M. L. (1981).

aperture of an antenna by benefitting from the motion of the vehicle the radar system is attached to, called Synthetic Aperture Radar (SAR).

### 3.2. Synthetic Aperture Radars

Synthetic aperture radar systems are used to produce images over a large desired area. Traditional radar systems employ a fixed location ground antenna, while SAR antennas are usually attached to an aircraft, and pass over a target region. The motion of the antenna makes its aperture synthetically large, increasing the radar system's max range [3]. Two antennas are typically used in a SAR system so that the angle of the receiving antenna is ideal to have the largest effective aperture. Figure 2 shows the basic concept of increasing a radar system's aperture with a moving vehicle and two antennas:

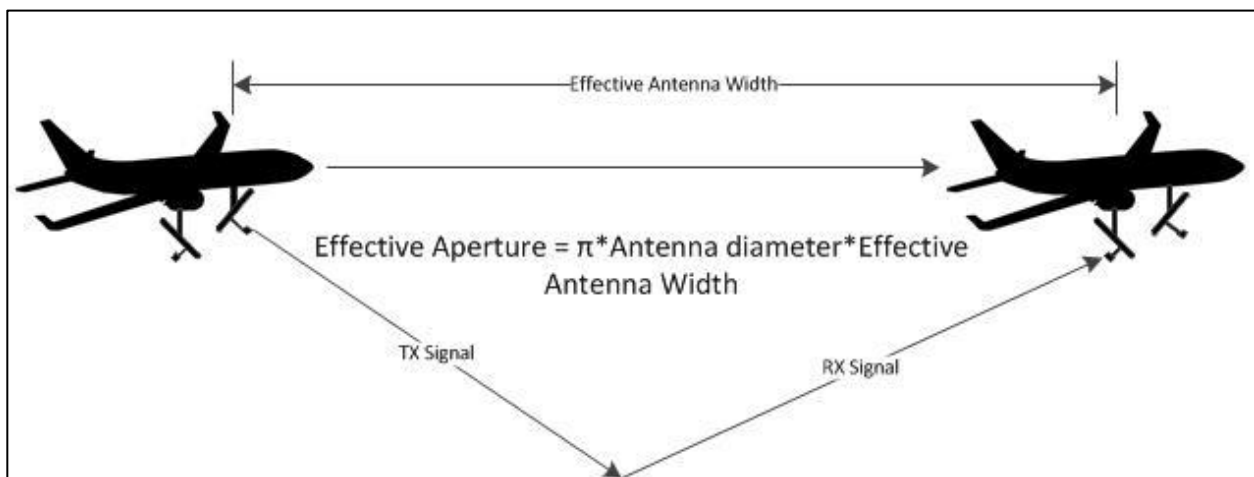


Figure 2: Synthetic aperture value.

By comparing the differences between the sent and received signal, the distance from the radar to the area being mapped can be calculated [4 p.703]. The radar for this project will use a Linear Frequency Modulated (LFM) chirp waveform as its signal. An LFM chirp waveform is a pulsed signal that has its frequency swept linearly across the width of the pulse [3 p.111]. The formulas for the sent and received signals are shown below:

$$\text{Sent Signal: } A_{tx} \left\{ \cos \left( 2\pi \left( f_{base} + t \frac{m_p}{2} \right) t \right) \right\}, \text{ for } t > 0$$

$$\text{Received Signal: } A_{rx} \left\{ \cos \left( 2\pi \left( f_{base} + (t - t_{echo}) \frac{m_p}{2} \right) (t - t_{echo}) \right) \right\}$$

for  $(t - t_{echo}) > 0$ ,  
 $A_{rx}$  is proportional to  $A_{tx}$  and the RX antenna gain

The pulse slope is defined as:

[2] Sandia National Laboratories. (2014).

[3] Mahafza, B. R. (2013).

$$\text{Pulse Slope: } \frac{B}{t_{\text{delay}}} = \frac{B}{\frac{R_{\text{nominal}} + R_{\text{swath}}}{c}} = \frac{B \cdot c}{2(R_{\text{nominal}} + R_{\text{swath}})}$$

The pulse slope is used to calculate what the pulse width will be, along with the operational bandwidth. The pulse width is the amount of time it takes to transmit the signal. Another important parameter is the time duration between the start of a new pulse after the previous pulse has started to be transmitted. This parameter is dependent on the resolution requirement for the radar. Depending on how accurate the radar needs to be, a new pulse may have to be sent before that old pulse has finished transmitting. If a new pulse does not need to be sent before the end of the previous pulse, then it will be sent immediately after the previous pulse is finished being sent. The formulas for pulse width and time between transmissions are shown below:

$$\text{Pulse Width: } \frac{B_{\text{operational}}}{m_p}$$

$$\text{Time Between Transmissions: } \frac{r}{c}$$

One of the key parameter for a synthetic aperture radar system is Noise Equivalent Sigma Naught ( $NE\sigma_0$ ).  $NE\sigma_0$  is the sensitivity level of a SAR system. It is the normalized radar cross-section where the dB level of the desired frequency range's power in the final image is equal to the noise power in the signal (a Signal to Noise Ratio of 1). The formula for  $NE\sigma_0$ , taken from an IEEE Derivation is shown below[5]:

$$NE\sigma_0 = \frac{4(4\pi)^3 d^3 K B T_{rx} N L_{\text{total}} \rho_a \sin(\theta_{\text{incidence}})}{P_{tx} \tau G_{tx} G_{rx} \lambda^3 c W_a}$$

Because the Ku-band (12-18 GHz) has such high frequency levels, it consequently has low wavelengths. The propagation loss of a signal during transmission is dependent on the wavelength of the signal. The smaller the wavelength, the more power is lost. The formulas used for propagation loss are shown below:

$$\text{Friis' Transmission equation: } \frac{P_{tx}}{P_{rx}} = G_t G_r \left( \frac{\lambda}{4\pi 2R} \right)^2$$

$$\begin{aligned} \text{Propagation Loss: } L_p &= 10 \left\{ \log \left( \frac{P_{tx}}{P_{rx}} \right) \right\} \\ &= -G_{tx} - G_{rx} - 20 \log \left( \frac{\lambda}{4\pi} \right) + 20 \log(2d) \end{aligned}$$

For an example, if a signal is in the middle of the Ku-band (15 GHz), with 15dBi gain antennas, and the target is 500ft away, in dB the propagation loss would be:

$$-15\text{dB} - 15\text{dB} + 55.96\text{dB} + 36.85\text{dB} = \underline{62.81\text{dB loss}}$$

---

[4] Calabrese, D., & Episcopo, R. (2014). pgs (1-4)

With a dB loss of 62.81dB, the Tx and Rx amplifiers have to be ample to amplify the signal to at least past the point where the SNR = 1, without adding in too much additional noise to the system. The actual dB loss would be even greater since Friis' equation does not take into account dB loss from the signal reflecting off of a surface. In lower bands with longer wavelengths, the propagation loss is significantly less, so the radar can be significantly less sensitive than a Ku-band's radar.

Since the frequencies used by the radar are in the 16.2-17.3 GHz range, the signals cannot be easily converted from analog to digital with enough resolution. The software defined radio (SDR) can only sample an input signal at 100 Mega-samples per second (MSPS), corresponding to a sample frequency of 100 MHz. The frequency of the received signal will not be able to be sampled by the SDR. To solve this issue, stretch processing is used.

### 3.3. Stretch Processing

Stretch processing mixes the sent and received signals and then filters the mixer's output signal to get a difference signal. By making the slope of the pulse's frequency with respect to time relatively low, the frequency difference between the two signals can be made small enough to get the desired resolution from the radar. The difference signal's frequency is defined as:

$$\begin{aligned} \text{Difference Signal Frequency: } f_{tx} - f_{rx} \\ &= f_{base} + t(m_p) - (f_{base} + (t - t_{echo})m_p) \\ &= t_{echo}(m_p) \end{aligned}$$

The resulting signal from the mixing and filtering will have the formula:

$$\text{Difference Signal: } A_{rec}\{\cos(2\pi t_{echo}(m_p)t)\}$$

Figure 3 shows the basic idea of stretch processing. The difference signal is passed through the ADC and is used to calculate the distance from the target to the radar. Because the slope of the sent waveform's frequency with respect to time as well as the pulsed signal width is known, it is possible to calculate the distance away a certain target is.

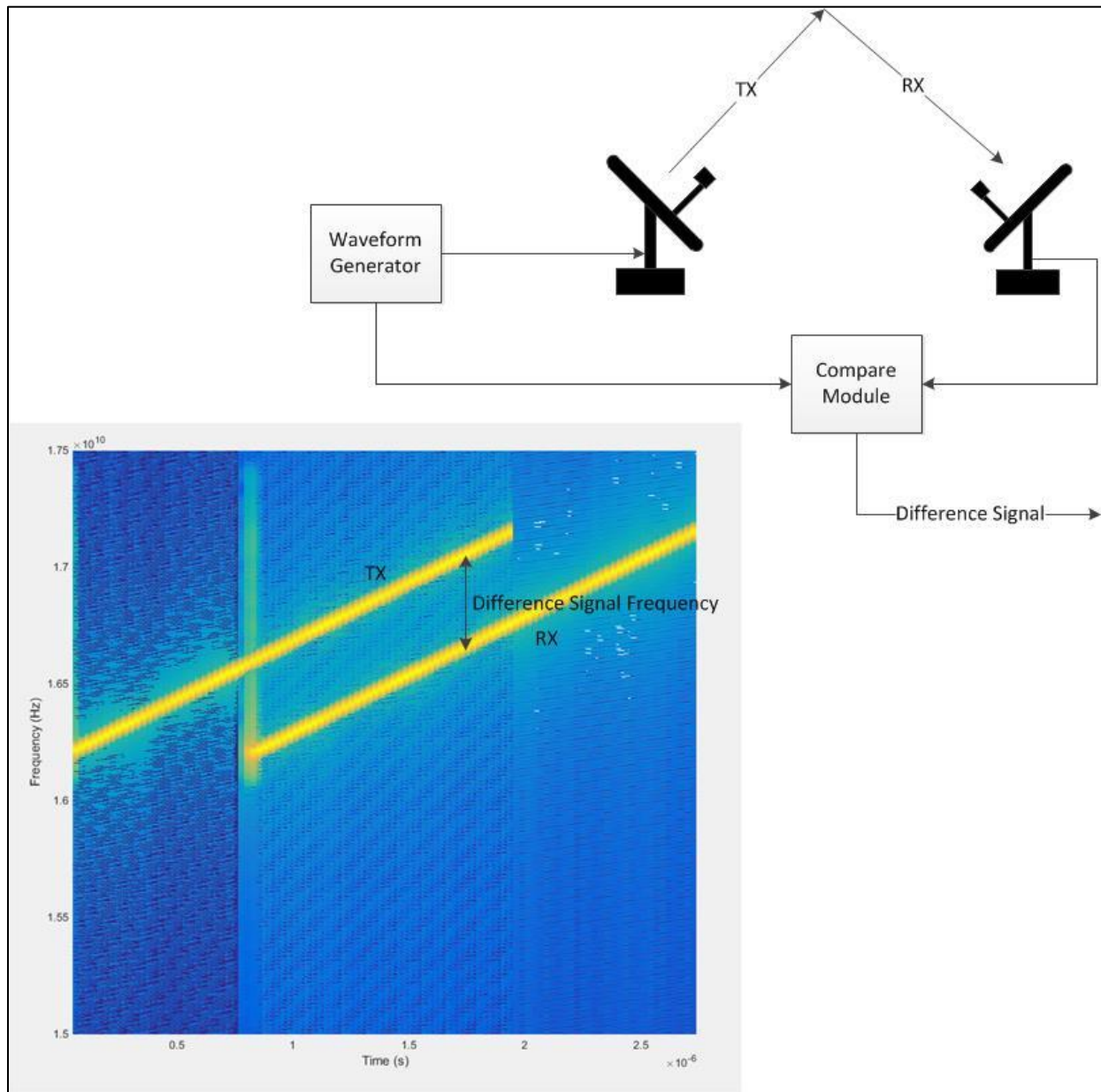


Figure 3: Stretch processing.

By using the frequency values of the difference signal along with the known frequency slope of the sent signal, the time it took the signal to be received (time delay) can be calculated. The time delay is multiplied by the speed of light, divided by two, and multiplied by the cosine of the angle of the receiver with respect to the ground to get the distance away from the target [2 pp.247-249]. The calculations are shown below:

Difference Signal Frequency:  $t_{echo} * m_p$

Time Delay:  $\frac{f_{difference\ signal}}{m_p} = t_{echo} = 2 \frac{d}{c}$

Distance to Target:  $\frac{t_{echo} * c}{2}$

True Distance to Target:  $d\{\cos^{-1}(\theta_{rx})\}$

For stretch processing to work, the sent and received signals need to have linear frequency sweeps and very little noise in the desired frequency range. Both of these issues were present in the previous radar and will be improved upon by this project's new radar design. One of the desired uses for the radar system designed by this project is to conduct proof of concept tests for a bistatic synthetic aperture radar system.

### 3.4. Bistatic Radars Testing

A bistatic radar system operates with separated transmitting and receiving antennas. Since SAR's normally operate on aircrafts, a bistatic SAR (BISAR) would have the transmitter on one aircraft, and the receiving antenna on the other. Splitting up the transmitter and receiver has many benefits. Separating the transmitter and receiver allows for the transmitter, which because of the power supply required to operate it is much heavier than the receiver, to be flown on a separate aircraft. The lighter receiver can be flown on a much smaller, more maneuverable aircraft. Some of the countermeasures that are used to make SAR data collection ineffective can be less damaging to a BISAR. A BISAR can also be better at distinguishing targets from clutter. If the transmitter is not on the same platform as the receiver, then it is also possible to have more than one receiver. While the actual processing of the collected data is more difficult with more receivers, the resulting images would be more detailed and accurate [6]. The development of algorithms for processing data from many different moving receivers from a single transmitter that is also moving will need to be tested with an accurate and powerful instrumentation radar system.

Group 105 wants to conduct proof on concept experiments to test the feasibility of implementing an accurate BISAR by testing with the radar system to be developed by this project. Other than the already mentioned technical benefits, BISAR's can have tactical advantages when being used in active combat areas, or conducting covert operations. By having the transmitter separated from receiver(s), the risk of a receiver being detected is lowered. It would be possible to have the transmitter be a space-based craft or very high altitude aircraft with small piloted aircrafts or UAV's in the area collecting data without having to transmit a signal, making them harder to detect [7]. Development and research of BISAR's could make collection of data on enemy's location safer and more accurate.

---

[6] Yarman, E., Yazici, B., & Cheney, M. (2008). pg 1

[7] Gierull, C. (2004). pg 1

## 4. Methodology

The objective of this project was the re-design of Group 105's current Ku-band SAR as a chassis-based Ku-band SAR that will be optimized for use as an instrumentation radar system. The project consisted of the following objectives:

1. Creation of a fully functioning Ku-band SAR operating at the specifications given by Group 105.
2. Designing detailed CAD and system models of the radar.
3. Collecting test data and analysis of the test data.

This project took place at MIT Lincoln Laboratory. The parts used to create the chassis based SAR system were either already owned by Group 105, or were ordered shortly after the start of the project. The test data was collected from on top of the parking garage at MIT Lincoln Laboratory with the radar system stationary. The following sections provide details for how the project objectives were completed.

### 4.1. Creating a Ku-band SAR System

The process of creating the radar system started with initially selecting components based on parts available at the lab. These parts were then tested to verify that the components would fulfill the requirement for the radar. The radar design was revised based off of the test data and then tested again. This iterative process continued until a final radar design was created that met the requirements of the project. Because of the short time period of this project, the radar system was designed around parts already in Group 105's possession. Each component had to be tested to check that it would satisfy the role that had been selected for it in the radar, and new components were added as necessary. After the radar had been assembled, the waveform used by the system had to be measured in a controlled lab space to verify that it met the required specifications.

#### 4.1.1 Selecting Initial Components

The first step of this project was to create an initial parts list and design for the SAR. To finish building the radar with enough time to collect and analyze data at the end of the project, the parts were limited to parts already at MIL LL with a few exceptions. The main exception was the Euvis arbitrary waveform generator, which was used to create the LFM chirp. It was chosen because of its high output sample rate (2.5 Gsps according to the specifications sheet). Having a high sample rate was necessary to meet the resolution requirements of the SAR. The SAR needed to have a resolution of 6 in. To meet this requirement, the LFM chirp would have to step to the next frequency level before the time it takes light to travel 6 in:

$$\frac{(0.5ft * 0.3048m/ft)}{(3 * 10^8 m/s)} = 508ps$$

In order to change frequencies faster than 508ps, a sample rate of the waveform generator would have to be faster than 1.97 Gsps (1/508ps). Since the Euvis AWG has a sample rate of 2.5 Gsps, it would be able to meet the resolution requirement. The waveform generator was ordered within the first week of being at Lincoln Labs. Once given the initial list of parts available for use in the project, the parts were inventoried. Table 2 contains the list of parts including the Euvis AWG.

Part Number	Manufacturer	Description	Quantity
DSM303	Euvis	Arbitrary waveform generator	1
HMC-C051	Hittite	DBL-BAL Mixer Module, 11-20 GHz	1
7ED20-8125/U-1250-O/O	K&L Microwave	Bandpass filter 7.5-8.75 GHz	1
CA618-5005	Ciao Wireless	29dB Amplifier 6-18GHz	1
1-10	Weinschel	10dB Attenuator	1
1-4	Weinschel	4dB Attenuator	1
HMC-C056	Hittite	X2 Active Frequency Multiplier 8-21 GHz	1
YL-92	Aeroflex	2 Way In-Phase Power Divider 12-18 GHz	1
15EDX10-16250/U2500-O/O	K&L Microwave	Bandpass filter 15-17.5 GHz	2
USRP N210	Ettus Research	Software Defined Radio	1

Table 2: Initial parts list.

The initial design for the SAR did not include any attenuation or isolation (except for a known isolation stage before the difference signal was created) parts, as the first goal was to create a bare bones design that could be added to and improved easily. The design required parts that had not been accounted for yet but were owned by Group 105.

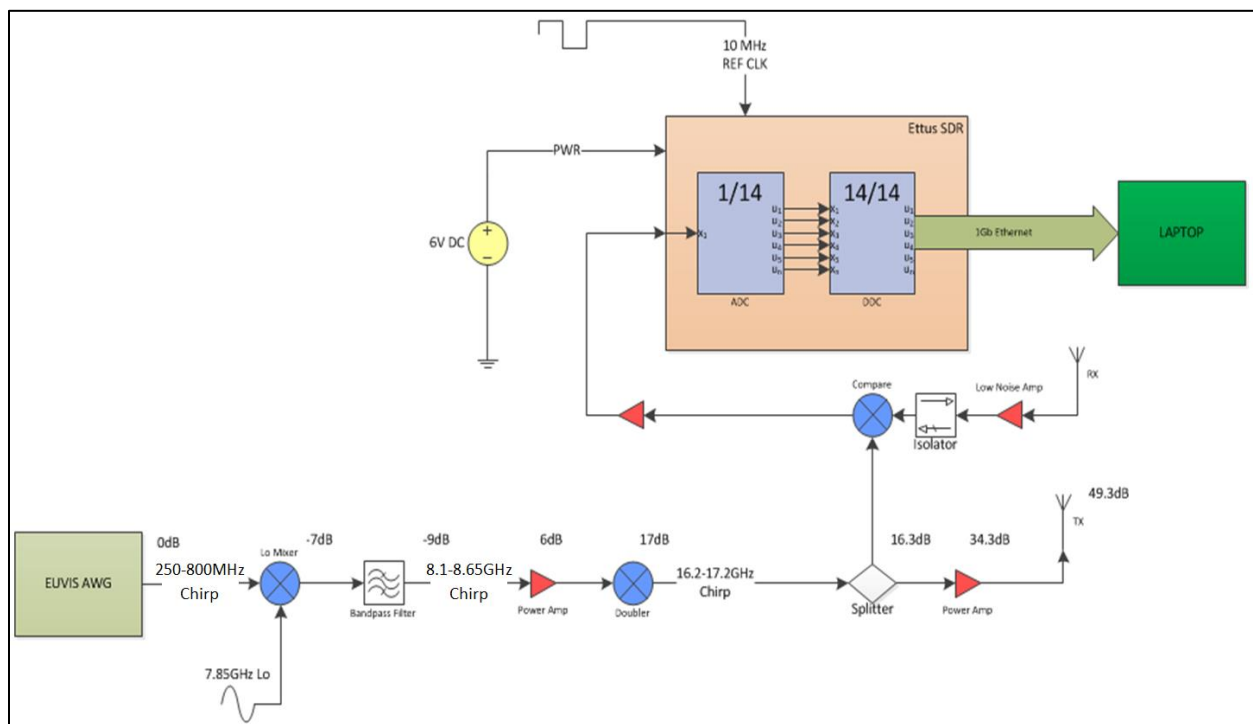


Figure 4: Initial design block diagram.

The initial block diagram (shown above in Figure 4) had the following parts assigned to various modules:

Part	Manufacturer	Module
HMC-C051	Hittite	Lo Mixer
7ED20-8125/U-1250-O/O	K&L Microwave	Bandpass Filter
CA618-5005	Ciao Wireless	Power Amp
HMC-C056	Hittite	Doubler
YL-92	Aeroflex	Splitter

Table 3: Initial parts selection.

Each state of the transmitting module was assigned a dB level that reflected change in power through the module. A power amplifier was placed between the bandpass filter and the doubler module because the doubler has a dB in requirement of 6dB.

The LFM chirp was given a range of 250-800 MHz because the AWG digitizes at a rate of 2.5 Gsps, limiting the frequency output to the Nyquist rate of 1.25 GHz or less. The frequency range would need to be converted to the desired 16.2-17.3 GHz. To convert the chirp, it was decided that the signal would be mixed with a 7.85 GHz wave and then doubled with a frequency multiplier.

After checking the specification sheet, it was determined that the HMC-C051 could not act as the Lo Mixer, as the Lo input for the part required a frequency between 12 and 20 GHz. The HMC-C051 was changed to be the mixer for the “Compare” stage of the design and a M2-0220 mixer module provided by the lab became the new “Lo Mixer” module component. It was also decided to add a 15EDX10-16250/U2500-O/O bandpass filter to both parts of the “Splitter” module’s output, to clean the signal before transmission and being used in the mixer. To make sure that these initial parts would work for their assigned stages; the first half of the transmitter (up until the frequency multiplier) was tested using a function generator and a spectrogram.

#### 4.1.2. Component Testing

After the initial design of the radar was decided on, the components to be used in the radar needed to be tested. As many of the parts were not yet accounted for during the initial phases of testing, function generators were used to simulate the waveform generators that would be added later. The function generator connected to the IF input to the mixer was set to have a frequency of 500 MHz with a sampling frequency of 1.25 GHz instead of using a frequency sweep, so it would be possible to read the frequency and dB levels at each stage of the radar design. The frequency and power levels of the signal at each stage of the system were checked with a spectrum analyzer. As each component was checked, parts such as attenuators were added to control the power level of the signal at each stage of the radar system. If it was discovered that a chosen part was not the correct choice for a certain stage of the radar, it would be replaced by a better suited part, and the stage would be tested again.

Because the majority of the testing was performed inside Group 105’s lab space, the radar system was tested without antennas at first. To simulate a signal being sent and received with antennas, a 10m long cable was used. Using a network analyzer, the cable was measured to have an 118.3ns delay. Once the frequency and power outputs of every stage before the compare module’s mixer was verified,

the input signal was changed from a constant frequency to an LFM chirp. Since the mixer would have an output signal of the difference between the LO and RF signals, the output would be zero if a constant tone was used. The frequency measured from the oscilloscope would be used to calculate the time delay of the wire and be checked against the time measured from the network analyzer. The function generator connected to the IF input to the mixer was controlled by a Matlab script originally created by a member of Group 105 that was altered to output an LFM chirp. The function generator was used until the AWG arrived to the lab.

The next component that could be tested inside the lab was the Ettus software defined radio (SDR). The SDR was selected to be the analog to digital converter and send the data over Ethernet to a laptop. The waveform sent to the radar system was controlled by the Euvis AWG at this point in the project. The AWG created a LFM chirp, the same as the previous test. The data sent to the laptop was analyzed using Matlab, generating an FFT graph of the signal. The frequency peak recorded by the SDR was compared to the calculated expected value as well as the value recorded by the spectrum analyzer to test the SDR's accuracy.

The next measurement taken was the power level of the signal after the power amplifier (PA). The radar system needed to have an output power before the antenna of 1 Watt (30dB). To measure the output power, a constant frequency tone was generated by the EUVIS AWG. The output from the PA was attenuated by a -35dB high power attenuator and measured by a spectrum analyzer. The signal was attenuated because the desired 30dB signal is outside the safe input power level for the spectrum analyzer. The attenuator values used at different points in the radar design were altered as needed to generate the desired output power level.

The final parts of the radar to verify were the low noise amplifier (LNA) connected to the receiver antenna, the 14 MHz filter after the mixer, and the variable attenuator placed right before the SDR. Again a constant frequency tone was generated. This would act as the Lo mixing signal to lower the frequency of the output of the LNA to be fed into the SDR. A function generator was connected to the input of the LNA, generating a -30dB signal with a frequency 13 MHz less than the frequency of the Lo signal. An FFT graph was generated from the signal recorded by the SDR and the frequency with the highest power level was displayed. It was necessary to verify the highest power frequency recorded was 13 MHz, that the noise levels were minimal, and that the variable attenuator was able to raise and lower the power level of the signal. Once all of the components of the radar system, other than the antennas had been verified, the output waveform of the radar needed to be measured.

#### **4.1.3. Waveform Lab Testing and Measurements**

After the radar had been designed and assembled, the waveform output of the system as well as the input to the SDR needed to be measured. These measurements were recorded in the lab, as the data collected later on in the field would have noise caused by clutter in the radar system's target range. The 118.3ns delay cable was not used to test the accuracy of the waveform. Instead, a high frequency oscilloscope was used to collect the data.

The main value of interest from measuring the waveform with the oscilloscope was the range sidelobe power levels. The waveform was generated by the radar and fed into the oscilloscope just after the power amplifier. The waveform was captured by the oscilloscope at 60 Gsps and analyzed by a member of Group 105 with Matlab code that had been previously created to measure similar data from the existing SAR system. Once the waveform had been measured and the components of the radar had been tested, data collection from on top of the MIT Lincoln Laboratory parking garage could begin and the models of the radar system could be created.

## 4.2. Radar Model Design

To help facilitate future work based off of the results of this project, digital models of the system were created to keep record of the final design of the radar system. If the radar system needed to be changed later on to fulfill a different role, the models will not only be a record of the past design, but can show the different changes made to the system over time. A 3D CAD model as well as a system block diagram model was made during this project.

After the final radar design was determined from testing the components, a system level block diagram was created. The model showed the connections between parts as well as the power requirements of different parts in the system. The system model was a continuation of the basic block diagram that was created at the beginning of the project, changing the design and adding parts when the results from testing showed a need for change. The final system model will serve as a way to catalog the parts used for the radar as well as document changes made in the future. If the radar system is ever changed, this model will be a record of past designs in case a previous design has to be recreated.

A 3D model was created for each component. These models were put together to create a digital assembly of the radar system. While most of the parts had to be modelled during the project, the Acopian power converters had pre-created models that could be downloaded from Acopian's website. The dimensions for each part, not including the custom filters used, were found from the specification sheets available on each part's supplier's website. Because the K&L microwave filters are custom made to fit the requirements of the buyer, there were no dimensions available online. These parts were instead measured to get the values for their models. The final assembly of the radar system did not show how the components were wired to the power sources. The goal of the model was to have a clean view of how the radar system should be laid out. The wiring of the individual components can be seen in the system model and used if the radar ever needs to be rebuilt. The SMA connections between the components were shown, however. This model will allow the physical radar system to be changed without having to worry about being able to reassemble the system at a later point in time.

## 4.3. Field Testing, Data Collection, and Analysis

In order to test the capabilities of new radar system, it had to be tested. Since it would not be possible to get an aircraft to fly the system, due to time and cost constraints, the parking garage at MIT Lincoln Laboratory was used. The data collected from these tests were then analyzed to judge the success of the radar design and the project. Two tests were performed during this project; targeting one stationary corner reflector target and one moving corner reflector target.

#### 4.3.1. Stationary Corner Reflector Test

The first test that was conducted was a simple check to make sure the radar was functioning properly. A corner reflector target was placed in the radar system's target range (See Figure 5). Corner reflectors have high radar cross-section values, making the return power received by the radar from the target significantly higher in magnitude than other objects in the radar's view. The distance was then measured with the radar system. Both the target and the radar were stationary, as this test was only to check that the radar had been built correctly. The data collected by the SDR in the system was transferred in real time via the Ethernet link to a laptop where it was analyzed in Matlab. The FFT function in Matlab was used to generate an array of frequencies. This array was graphed and the max value was found with a simple loop search. Based on the peak frequency and the slope of the pulse, the distance to the target was calculated. After the accuracy of the radar was verified with this test, the radar was used to track a moving target.

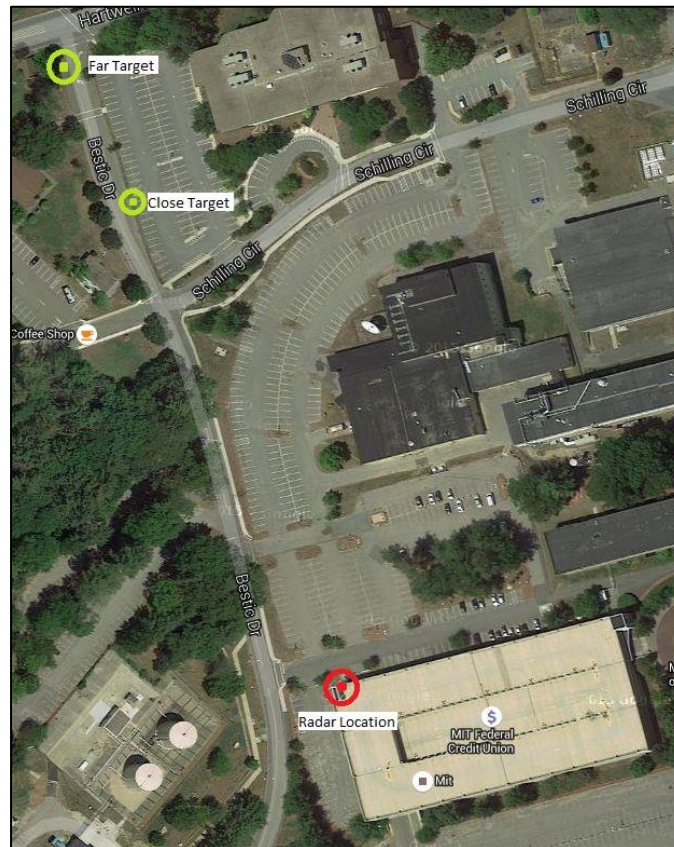


Figure 5: Stationary targets.

#### 4.3.2. Moving Corner Reflector Test

The next test was more complex. While the radar system was again stationary, the corner reflector was driven through the radar's view (See Figure 6). FFT's of small sections of the dataset were generated and graphed, refreshing with each new section of data. The resulting graph showed the changing frequency of the peak with respect to time, corresponding to the changing distance of the target to the radar. This test will show the full range of the radar, which will be limited by the bandpass

filter after the “Compare” module of the radar as well as the laptop used to collect the data. Since the SDR transmits the data to the laptop at 50 Msps, the signal will have to be decimated so that the laptop can write the data to memory. If the signal is not decimated, it is possible that the laptop will take too long to write the data of one packet, causing data from the next packet to get overwritten and lost before the next time the laptop tries to write the data. The decimation value will depend on the specifications of the laptop, notably the speed of the processor as well as the speed and amount of the memory. For example: a decimation value of 4 will result in only 12.5 Msps of data to the laptop, resulting in a sample rate of 12.5 MHz. Since the real and complex values of the signal are recorded, the effective bandwidth of the radar is 12.5 MHz as well, as Nyquist rate limited bandwidths only apply to datasets without complex values. The bandpass filter used in the radar has a bandwidth of 10 MHz. While a decimation rate of 4 will allow for the full range of the radar to be recorded, a decimation rate of 8 would be too high. Using the Matlab toolkit developed by Group 105 during the previous summer, a ranged Doppler map was generated to display the target moving through the scene as well as the FFT graphs.

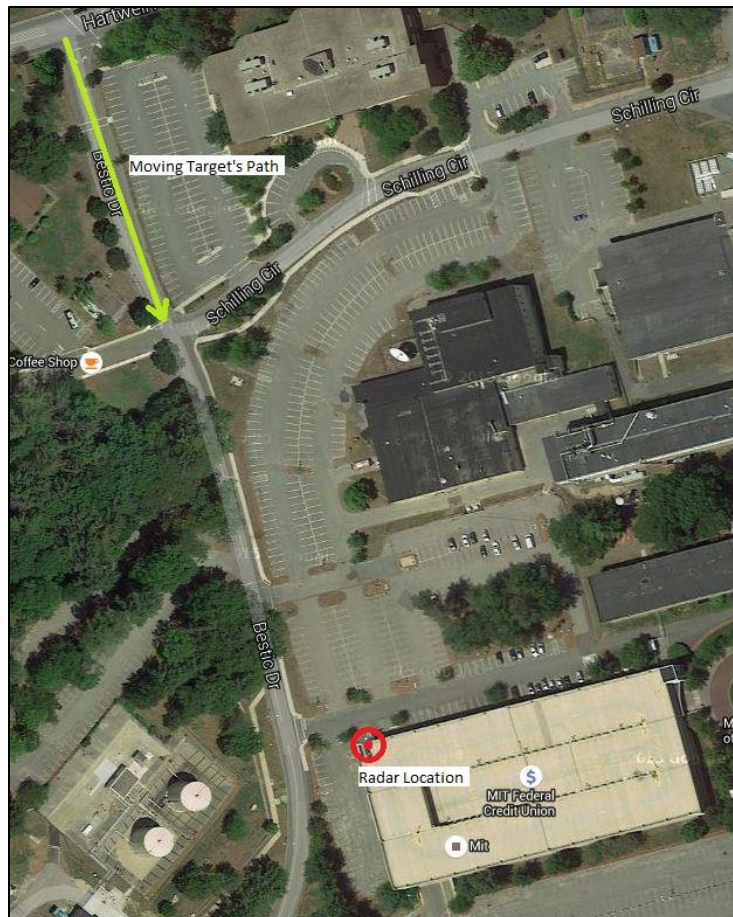


Figure 6: Moving target.

### 4.3.3. Analyzing the Test Data

Once the tests were complete, the same test data was analyzed using Matlab tools that were provided by Group 105, with minor alterations to correctly read in the test data. The performance metrics generated by the Matlab scripts were compared to the performance metrics measured from data collected by the existing SAR. Waveform linearity and instantaneous bandwidth were the two main parameters that the new radar system was designed to improve. A main gage of the success of the new radar design was how much improvement in these two areas the new system had over the existing system.

The tests performed with the new radar system were to determine if it had met the requirements set by Group 105. The radar had to have a resolution of 6 inches, a -30 dB gap between the main peak the point-scattered sidelobes, have a nominal range of 700 ft with a range swath of 300 ft, and a sensitivity level of -40 dB. All of these values could be determined by analyzing the data collected during the rooftop test as well as the data collected in the lab. The success of this project heavy depended on whether or not the requirements set for the radar at the beginning of this project were met. To succeed, the radar system needed to have a well thought out and planned system design.

## 5. System Design

There were three main changes made between the previous SAR, and this project's design.

1. Use of a Digital Arbitrary Waveform instead of an analog PLL waveform generator
2. Replacement of MMIC components with individual shielded modules
3. Use of a the receiver of a Software Defined Radio instead of a custom receiver module

The AWG was selected to improve the linearity of the system. The individual analog components, which will be connected with rigid SMA connectors, will decrease the noise generated in the signal from interference. By decreasing the noise in the signal, the usable instantaneous bandwidth should be increased from the previous model. The SDR has a 1 Gigabit Ethernet data output port to allow streaming and display in real-time of the collected data. The changes were decided by Group 105 before the start of this project, and were used as the starting requirements to design the SAR. After the initial requirements were determined, the initial set of parts was selected for the SAR. The initial design was then tested and revisions were made to the design based off of the test results. Eventually a final design was decided upon and built.

### 5.1. Final Components

Based off of the results of the lab tests that were performed, the radar system design was refined into its final iteration. The high-level system model (Figure 7) depicts the main subsystems used in the radar. Filters, amplifier, attenuators, and isolators were added into the system to meet dB input requirements and keep the signal clean.

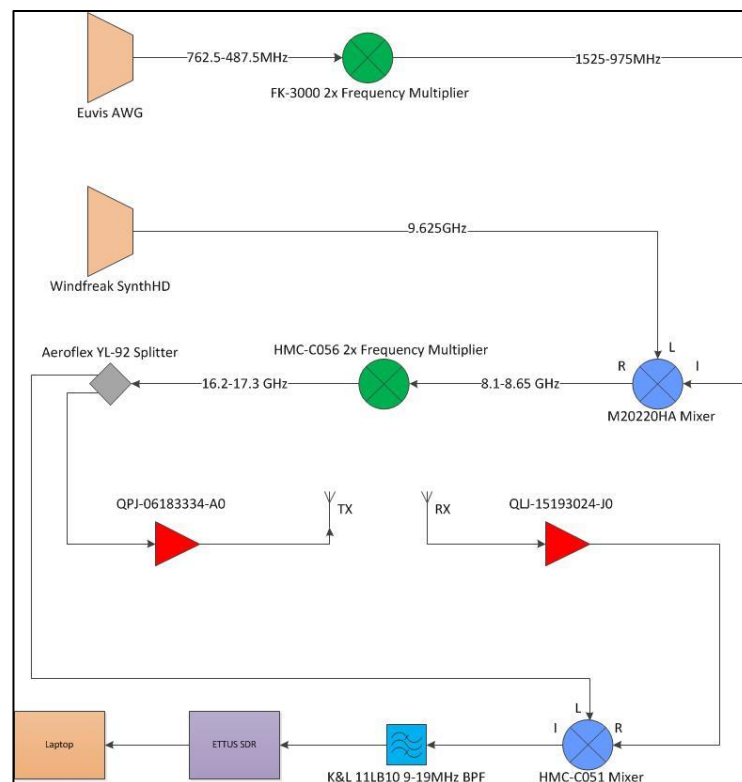


Figure 7: Final radar system model.

### 5.1.1. Output from the Reference Oscillator

Going through the testing process, many components were changed, added, or removed. Starting with the 10 MHz oscillator, its output was connected to the SDR as well as the Windfreak waveform generator (See Figure 8). Its output had to meet the dB input requirements of the waveform generator and the SDR. The signal needed to be amplified and filtered before being fed into a splitter. The AWG requires 10-12dB input and the SDR has a max input power level of 15dB. While the oscillator has an output power of 13dB, the splitter was measured to lower power by 3.6dB in the lab, causing the input power level for the waveform generator to be just below the required power level. The CA-515 amplifier was selected because it allows input signals of a minimum 13dB. The other available amplifiers in the lab would not have been able to handle the power level of the oscillator's output signal. The resulting signal needed to be attenuated 1dB before feeding into the waveform generator, as it was slightly over its tolerance threshold.

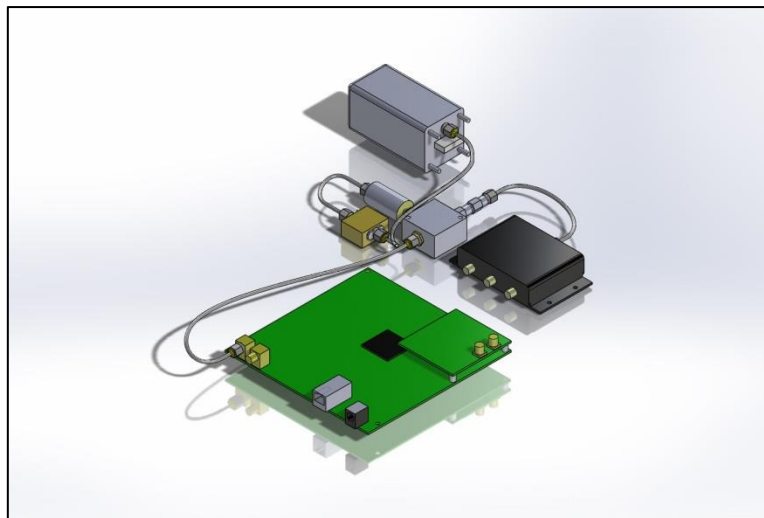


Figure 8: Oscillator connections.

Since the waveform generator has two output terminals, it was used as the reference clock to the AWG as well as the Lo signal to mix the signal into the RF spectrum. The Lo signal was filtered and amplified by a CA218-2004 amplifier to meet the M20220HA mixer's dB range of 13-22dB. The input to the Lo was measured to be 13dB in the lab. The original selection of the HMC-C051 mixer was replaced by the M20220HA because its minimum IF input frequency is 11 GHz. It was decided to use the HMC-C051 as the mixer to compare the signal from the receiver to the reference chirp taken before the power amplifier. The IF input signal to the M20220HA was driven by the AWG, but the signal had to be significantly altered to meet the frequency requirements of the radar system.

### 5.1.2. Waveform Alteration

The original waveform that was selected for the AWG to output was a 250-800 MHz LFM chirp. It was going to be mixed with a 7.85 GHz signal to generate an 8.1-8.65 GHz LFM chirp. This would be accomplished by taking the sum of the Lo and IF ports at the mixer. The resulting signal would be frequency doubled to get a final 16.2-17.3 GHz LFM chirp. The original frequency plan had to be changed however. The bandpass filter that was used after the RF port of the mixer to get the signal into the 8.1-

8.65 GHz range has a range of 7.5-8.75 GHz. Because of the lower limit of 7.5 GHz, the Lo signal of 7.85 GHz would not have been filtered out, causing unwanted frequency peaks in the signal at the final transmission stage. To solve the issue, it was decided to take the difference of the Lo and IF ports of the mixer, allowing the Lo signal to have a frequency greater than 8.75 GHz, which would be filtered out. The other option would have been to use a different filter, but it would have to be custom ordered and would have taken weeks to arrive. Because the difference of the Lo and IF signals would now be used, the bandwidth of the output signal out of the AWG would have to be half of the original value of 550 MHz. The minimum Lo signal value would have to be greater than 8.75 GHz, causing the minimum starting frequency for the LFM chirp to be greater than 650 MHz, causing the end frequency of the LFM chirp to be at least 1200 MHz. The EUVIS AWG has a clock rate of 2.5 GHz, resulting in a Nyquist value of 1.25 GHz. Because it would be desirable to have a Lo frequency of over 9 GHz to lower the power level of the Lo signal at the RF output port, the resulting end frequency of the LFM chirp would be over the Nyquist frequency. To solve this problem, the bandwidth of the LFM chirp was halved to 275 MHz. The frequency would be doubled before the M20220HA mixer to achieve the 550 MHz bandwidth. The lab already had a 975-1525 MHz bandpass filter (550 MHz of bandwidth) that would be ideal to clean the signal before the mixer. Since this filter was selected, the LFM chirp would have start and end frequencies equal to half of the filter's start and end values, resulting in a LFM chirp with a start frequency of 762.5 MHz and an end frequency of 487.5 MHz. The signal would be a down chirp because the difference of the Lo and IF ports would be taken. The higher IF frequency would result in a lower frequency value at the RF output port, resulting in the desired increasing LFM chirp at transmission. The Lo signal, outputted from the Windfreak function generator was set to 9.625 GHz ( $8.1 + 1.525 = 9.625$ ). After the waveforms for the radar system had been selected, the correct components for the radar could be selected.

### 5.1.3. AWG to M20220HA Mixer

The output signal of the AWG was measured to have a DC offset. To correct this, a BLK-18-S+ DC Block was added to the design. To get the input bandwidth to the M20220HA mixer's Lo port to 550 MHz, an FK-3000 2x frequency multiplier was added to the design. The input to the frequency multiplier needed to be 12-15dB in power. The ZX60-43-S+ amplifier was selected to amplify the AWG's output signal because of its frequency range (0.5-4000 MHz) and its max dB output level of 13dB. The signal had to be attenuated by 8dB before the amplifier to not overdrive the amplifier. To get the signal as clean as possible, three VLP-11+ 780 MHz low pass filters (LPF) were added in between the amplifier and the frequency multiplier. The AWG has harmonics that needed to be lowered as much as possible, so that they would not greatly affect the signal after the mixer. The LPFs removed the frequency peaks caused by the harmonics of the signal. After the frequency multiplier the signal was filtered again before being connected to the IF input of the mixer. The connections between the AWG, the Windfreak waveform generator, the M20220HA mixer, and all of the in between components are shown in Figure 9.

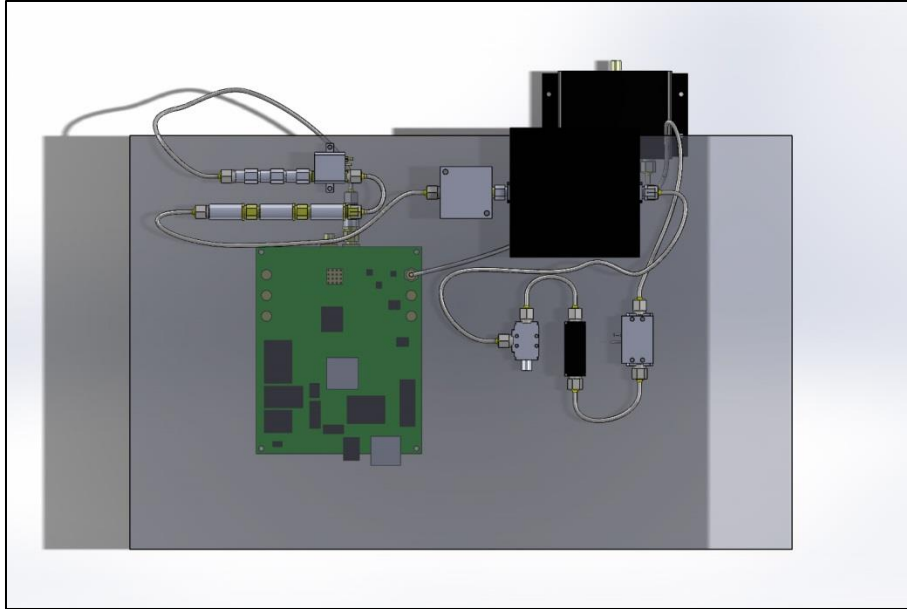


Figure 9: Lo and IF ports of the M20220HA mixer.

#### 5.1.4. From M20220HA through Transmission

Figure 10 shows the radar components used between the two mixers in the system. Between the two mixers, the frequency of the signal had to be doubled again and split to send to the power amplifier (PA) as well as the last mixer. To increase the bandwidth of the chirp to the desired 1.1 GHz, as well as shift the frequency of the signal into the Ku band, a HMC-C056 2x frequency multiplier was the next major component of the radar design. This was the same frequency multiplier that was selected in the initial design. The frequency multiplier has a required input power level of 6dB. An AML618P2501 amplifier was inserted between the frequency multiplier and the M20220HA mixer, which amplified the signal by 25dB. After the output from the mixer had been filtered, the power level of the signal was measured in the lab to be -12dB. 7dB of attenuation was added to lower the power to -19dB, resulting in the desired 6dB input power level to the frequency multiplier after amplification.

Now that the signal was the desired 16.2-17.3 GHz linear chirp, it was filtered and sent through an Aeroflex YL-92 splitter, going to the transmit antenna and the Lo input of the comparing HMC-C051 mixer. The final step before the transmit antenna is a QPJ-06183334-A0 PA. The PA has a gain of 34dB. Since the desired output of the PA is 1 Watt (30dB), the signal had to be attenuated. After the splitter, the signal was measured to have a power level of 8dB, as the frequency multiplier is rated to have an output power of 14dB on its specification sheet and the Aeroflex splitter lower the signal by 6dB. 12dB of attenuation was added after the splitter. A DITOM DF6701 Ku band isolator was added after the attenuators to help remove noise from the signal before the final amplification stage.

The Lo input of the HMC-C051 mixer has a required Lo input power level of 13dB. A CA218-2004 amplifier was used to amplify the signal from the other output of the Aeroflex splitter to meet this requirement. 6dB of attenuation was added before the amplifier to generate an output signal of 13dB, as measured by a spectrum analyzer in the lab. Just as before the PA, a DF6701 isolator was added after the CA218-2004 amplifier and before the Lo input of the mixer.

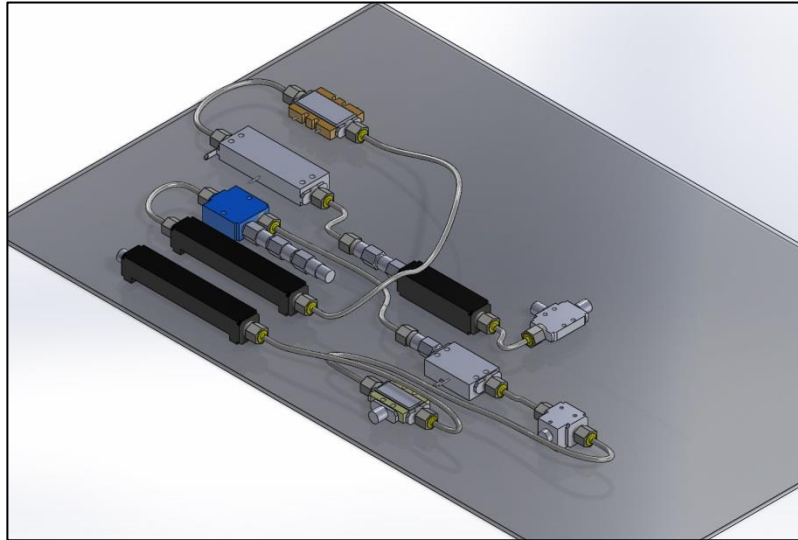


Figure 10: M20220HA RF port to the HMC-C051 mixer without the PA and LNA.

### 5.1.5. Receiving Path of the Radar System

Since the output signal of the mixer would be in the High Frequency (HF) radio spectrum range (3-30MHz), the IF port of the mixer was used as the output and the RF input port was used as the input. This configuration is the reverse of how the M20220HA mixer was set up. The RF port was driven by the signal from the receiving antenna, which was amplified by a QLJ-15193024-JO low noise amplifier (LNA) and filtered before being connected to the mixer. The output of the mixer was filtered, amplified by a ZX60-43-S+ amplifier, and passed through a H626 variable gain amplifier (See Figure 11). The variable gain amplifier has a mechanical dial that allows for tuning the amplification of the signal in the field as necessary before being fed into the SDR. After the signal reaches the SDR, it is converted to a digital signal by a 14-bit Analog to Digital converter, mixed with an Lo signal and decimated based on values set in the Matlab interface. The resulting array of complex values is transferred to the laptop via an Ethernet connection where the signal can be stored and analyzed.

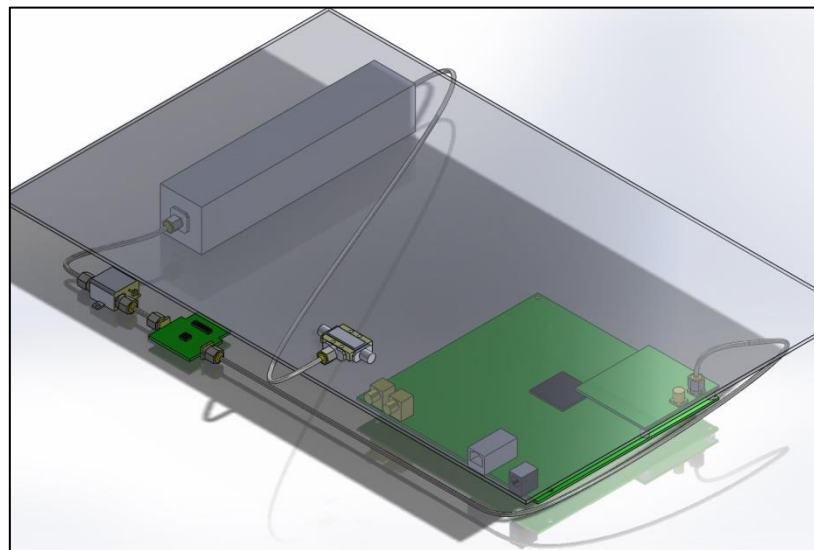


Figure 11: HMC-C051 mixer to the SDR.

## 5.2. AC to DC Converters

After all of the components were selected, AC /DC converters needed to be selected to meet the voltage and current requirements of the radar system. The Table 4 shows the voltage and current requirements for each part.

Part	Manufacturer	Voltage	Max Current Draw
SRS Oscillator	Stanford Research Systems	15 V	533 mA
CA218-2004 Amplifier	Ciao Wireless	15 V	200 mA
CA218-2004 Amplifier	Ciao Wireless	15 V	200 mA
M/A CA515	M/A-COM	15 V	130 mA
AML6182501	Microsemi	15 V	280 mA
QPJ-06183334	Quinstar	12 V	3.9 A
EUVIS AWG	EUVIS	12 V	0.75 A
HMC-C056	Hittite	+12 V, -5 V	102 mA (+), 5 mA(-)
QLJ-15193024-J0	Quinstar	6 V	0.170 A
Windfreak Synth-HD	Windfreak	6 V	1 A
ETTUS N210 SDR	ETTUS	6 V	1.3 A
ZX60-43-S+	Mini-Circuits	5 V	110 mA
ZX60-43-S+	Mini-Circuits	5 V	110 mA
H626	Hittite	5 V	225 mA

Table 4: Voltage and current requirements.

Based off of the above information and the AC/DC converters available at the lab, 6 Acopian converters were selected. Even though only four different voltages were needed, two 12 V and 5 V converters were used. The HMC-C056 requires a +12 V supply and a -5 V supply with a shared ground. These needed to be separate from the rest of the parts that used 12 and 5 volt converters. Three of the converters were already owned by group 105: two 5 V converters with currents rating of 2.5 A and 50 mA, and one 12 V converter with a current rating of 1.2 A. The other three converters were ordered from Acopian: one 12 V converter rated at 5.8 A, one 15 V converter rated at 2 A, and one 6 V converter rated at 5 A. With the power converters selected, the list of parts for the radar was complete.

## 5.3. Final Design and CAD Model

Once all of the parts for the radar system had been selected, it was build and digitally modelled. Most of the individual components, other than the custom filters, had specification sheets available online to find the dimensions of the part. The parts were modelled based off of the specifications found and the parts lacking a spec sheet were measured and modelled as well. After all of the parts were created, a digital assembly could be created with all of the parts included. Before the assembly could be created, the mounting points of the parts to the chassis had to be known. All of the parts were given to Group 107 where they were attached to the chassis. A second level for the radar system was also cut and had parts attached by Group 107 as well. Once all of the parts were attached to the chassis, the distances between the parts were measured and the final assembly of the radar as completed. The assembly did not include the PA, LNA, antennas, housing for the antennas, or the isolator attached to the PA because the housing used was only temporary used for testing purposes during this project. The

final system model, CAD design and actual radar system are shown in Figure 12, Figure 13, **Error!**  
**reference source not found.**, Figure 15, and

Figure 16.

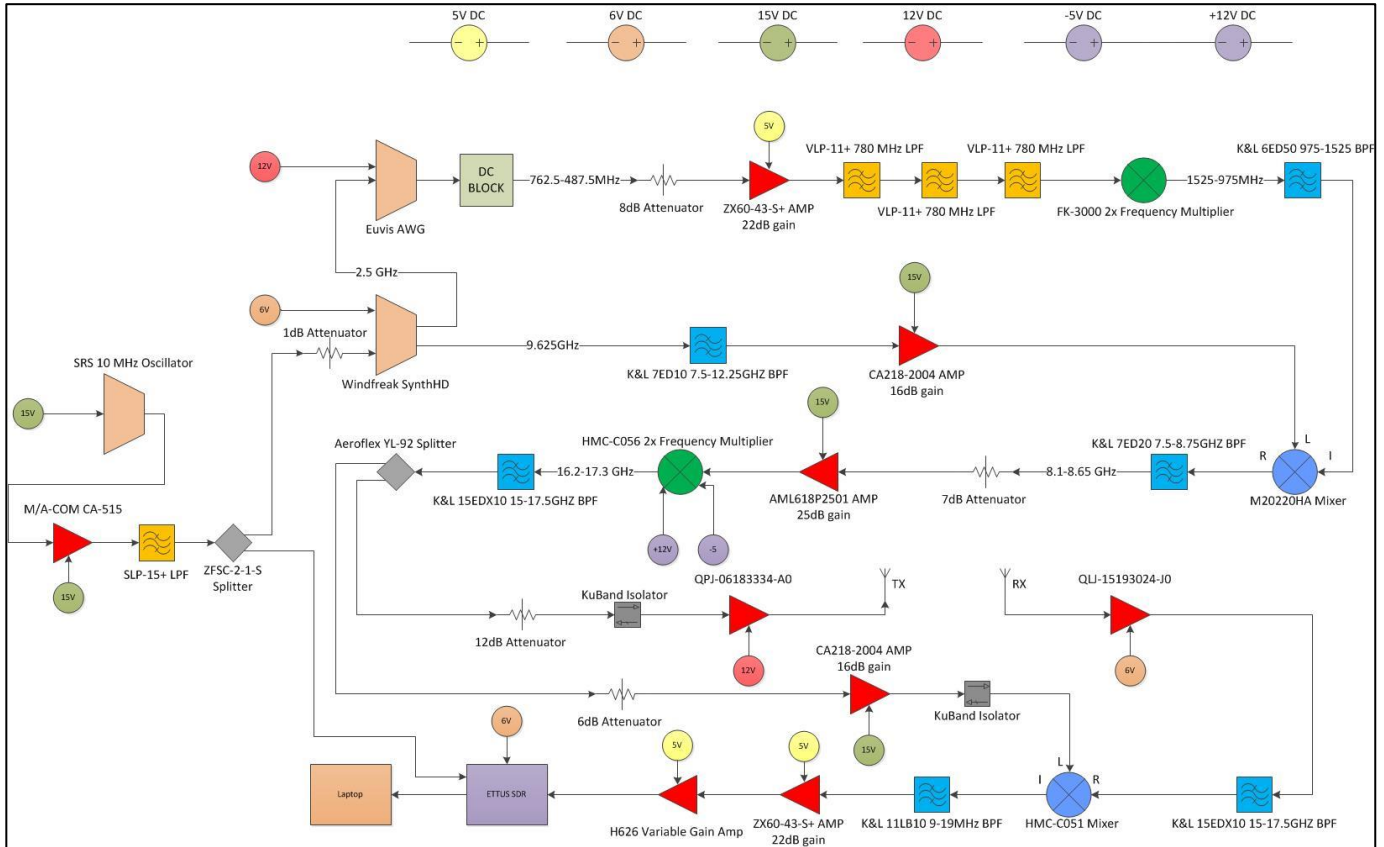


Figure 12: System model.

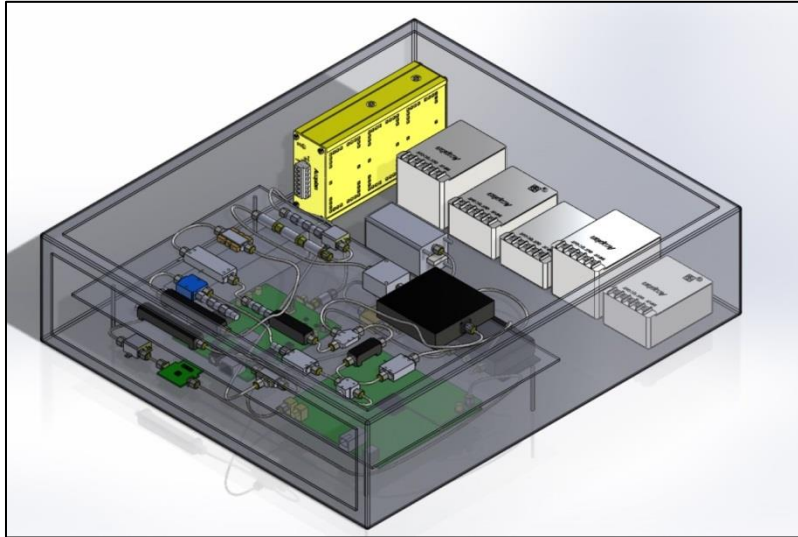


Figure 13: CAD model.



Figure 14: Final radar system design.

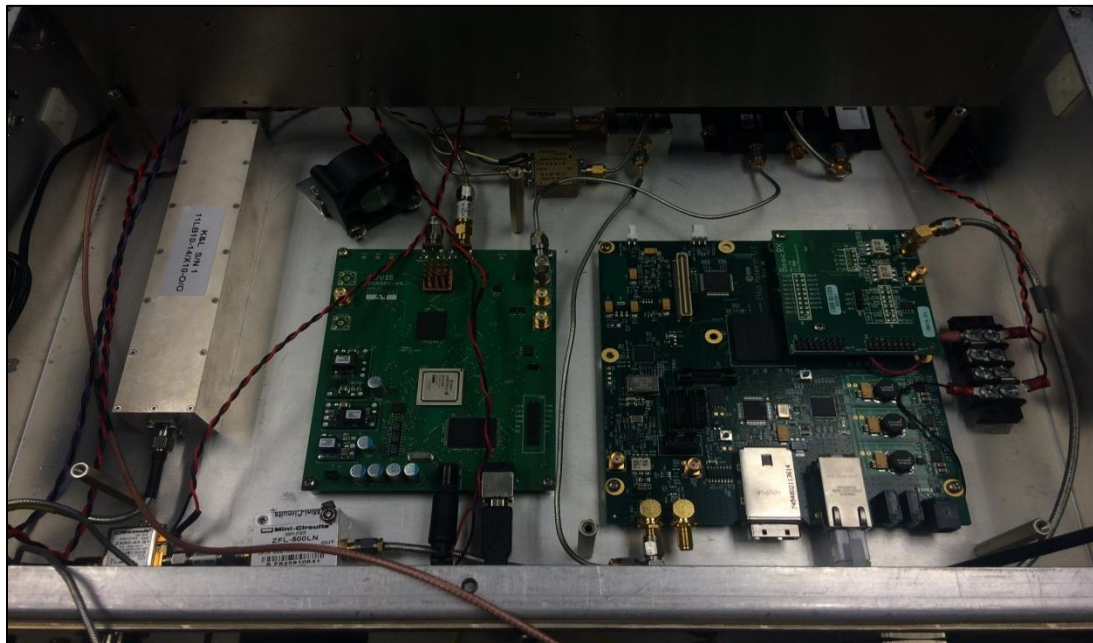


Figure 15: Lower level of the radar design.

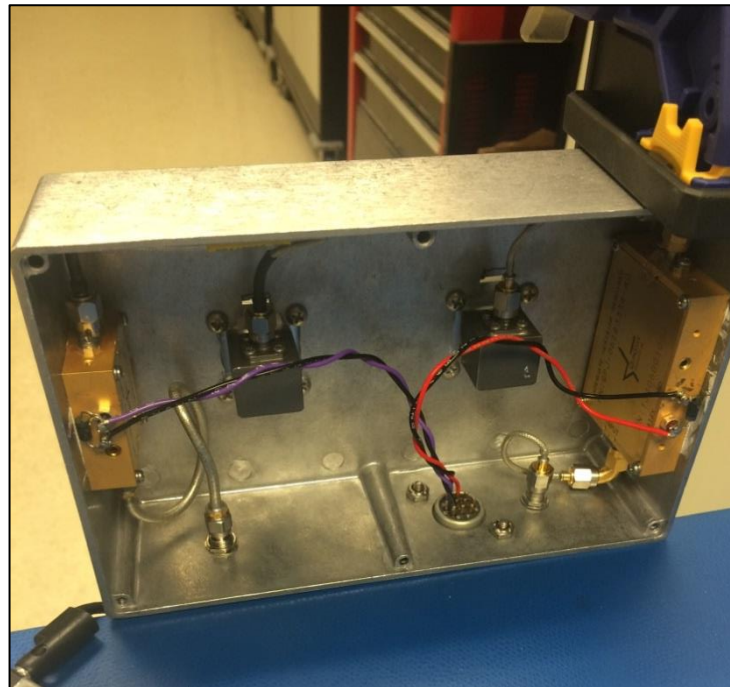


Figure 16: PA and LNA housing.

#### 5.4. Waveform Selection

After the radar design was complete, the waveform used by the radar had to be defined. As stated previously, the start and end frequencies would be 762.5 and 487.5 MHz respectively. The duration of the pulse still had to be determined, however. Because the center frequency of the final filter before the SDR is 14 MHz, the frequency gap between the transmitted and received pulses due to time delay should be close to 14 MHz in the middle of the range swath that the radar was being designed to cover. Group 105 will perform tests and data collections using this project's radar system at a range of 500 ft with the antenna positioned at a 45 degree angle (707 ft total distance). The calculations for the pulse width of the waveform are shown below:

$$\text{Time Delay: } 2 * \frac{d}{c} = 2 * \frac{(707) * 0.3048 \text{ m}}{3 * 10^8 \text{ m/s}} = 1.437 \mu\text{s}$$

$$\text{Pulse Slope: } \frac{f}{t_{\text{delay}}} = \frac{0.014 \text{ GHz}}{1.437 \mu\text{s}} = 9.74 \text{ MHz per } \mu\text{s}$$

$$\text{Pulse Width: } \frac{\Delta f}{m_{\text{pulse}}} = \frac{17.3 \text{ GHz} - 16.2 \text{ GHz}}{9.74 \text{ MHz per } \mu\text{s}} = 112.82 \mu\text{s}$$

To keep the received frequencies in the lower half of the filter's bandwidth for testing, it was decided to have 13 MHz correspond to 100 ft past the end of the range swath (907 ft). The corresponding desired pulse width was calculated to be 155.95  $\mu\text{s}$ .

The signal input to the SDR had to be decimated to allow the data to be stored by the laptop without data points being dropped. The laptop used was a 2011 Dell Precision M6400 with an Intel Core

2 Duo processor and 4 GB of RAM. Due to the lack in performance power of the laptop, the decimation value was set to 16. Because the signal being sent to the laptop was decimated, the number of samples from the AWG per pulse had to be divisible by the total decimation of the signal from the SDR. The SDR reads in signals at 100 Msps. Since the output from the AWG is 2.5 Gsps, the signal is initially decimated by 25. The resulting signal is then decimated by 16 to be able to be stored by the laptop, resulting in a total decimation of 400. The AWG was programmed via the GUI provided by EUVIS to step through a list of frequency values provided by an input file. The FPGA on the AWG board produces eight values at the 2.5 Gsps rate for each frequency specified in the input file. To meet the pulse width requirement, 49344 frequencies were used, starting at 762499999.8 Hz and ending at 487560813.8 Hz. The values are not exactly the desired start and end frequencies due to the analog to digital converter on the AWG being unable to output at those exact frequencies. The pulse width of this signal was 157.9us. To make the number of samples divisible by the total decimation value, a delay was added to the beginning of the waveform. EUVIS' GUI allows for a delay to be specified (in HEX) and is treated like an empty frequency value, having the AWG not output a signal for  $(8 \text{ samples} / 2.5e9 \text{ Gsps})$  times the delay value. 656 (0x290) delay addresses were added to make the total waveform have 400000 samples  $((49344+656)*8)$ . The total width of the waveform was 160us.

## 6. Results

The SAR system designed by this project had to meet specific requirements to be useful to Group 105 as an instrumentation radar system. Measurements such as the range and range swath of the system could be measured by analyzing the collected test data from the MIT Lincoln Labs parking garage. The cross-range sidelobe value was determined by analyzing data collected in the lab. Other metrics such as the system's resolution and sensitivity were calculated based off of values measured in the lab, as data collected from the parking garage will have noise from objects in the radar's target range. The parking garage tests were a good benchmark to compare against the existing SAR design, however. Both radars performed the same tests at the same location, and they can be compared through the differences in the data that was collected by both systems.

### 6.1. Lab Measurements

Before the radar system was brought to the parking garage and tested, measurements were taken in the lab to verify that output signal met the required parameters. A 60 Gsps oscilloscope was used to measure the output of the radar system after the power amplifier. Because the power level of the output signal was 1 Watt (30 dB), a high-power attenuator was inserted in between the amplifier and oscilloscope, preventing the high power signal from damaging the oscilloscope. Multiple pulses were recorded and saved to be processed in Matlab, allowing the values of the useable bandwidth and range sidelobe power levels to be measured.

The desired useable bandwidth of the system was the full 1.1 GHz. The previous radar design had only been able to use 500 MHz of its bandwidth because of non-linearity issues at the ends of the LFM chirp. Figure 17 shows the LFM chirp of one of the pulses recorded by the oscilloscope. The useable bandwidth of the measured pulse was 1.0923 GHz, a significant improvement over the previous design and almost reaching the full bandwidth of 1.1 GHz. The change in useable bandwidth can be attributed to the use of a digital arbitrary waveform generator instead of an analog PLL. Because the waveform generator used on the existing SAR system was analog, it could not immediately start a new LFM chirp after the previous one had ended, it had to take time to slow back down to the starting frequency before it could start again. To solve this issue, Group 105 had used two generators. One would start increasing frequency after the other one had ended. While this allowed for waveforms to be sent constantly, frequency errors would occur when the two generators approached the same frequency value (see Figure 18). Because of the high interference this caused, most of the beginning sections of the waveform could not be used, spoiling the resolution of the radar system. Because the AWG is digital, it can switch back down to the starting frequency without having to take time to reset. Now only one waveform generator is needed, removing the issues that having two generators interfering with each other caused.

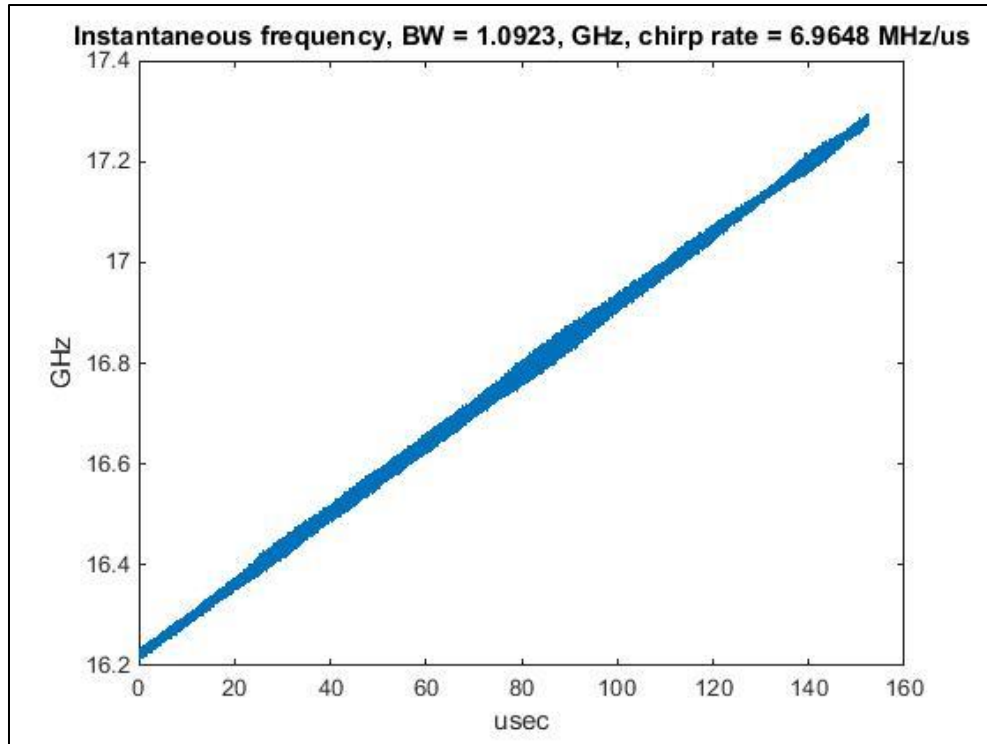


Figure 17: Useable bandwidth.

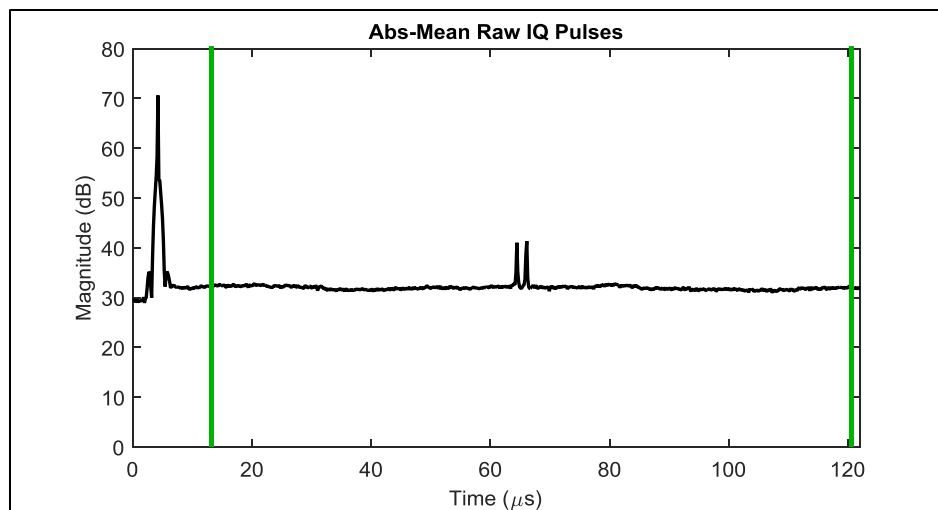


Figure 18: Interference from two generators from Christopher Panuski's presentation on LiTE SAR ground data collection.

The other value measured in the lab was the range sidelobe power levels (see Figure 19). The previous radar design had measured range sidelobe power levels of -20dB below the peak power level. Group 105 wanted this radar system to reach power levels of -30dB below the peak power level. This would give the radar a much cleaner signal and cleaner resulting SAR images, which is needed for an instrumentation radar system. Sidelobes can be caused by lingering intermodulated and harmonic signals that pass through filters without being attenuated completely. Having filters that match the frequency plan of a radar design instead of accepting other frequencies as well results in lower sidelobe

power levels. The range sidelobe power levels for this radar design are about 27dB below the peak power level, an improvement from the previous design but not completely meeting the required 30dB. One way to improve the radar system in future work is to replace some of the filters in the design with custom filters that exactly match the frequencies that need to pass through the system. Because this project designed the radar system with parts available at MIT Lincoln Labs, most of the filters accept frequencies other than the LFM chirp frequencies, resulting in higher sidelobe power levels. With the lab measurements complete and the radar system showing consistent performance improvements over the previous system, data was collected from the MIT Lincoln Labs parking garage.

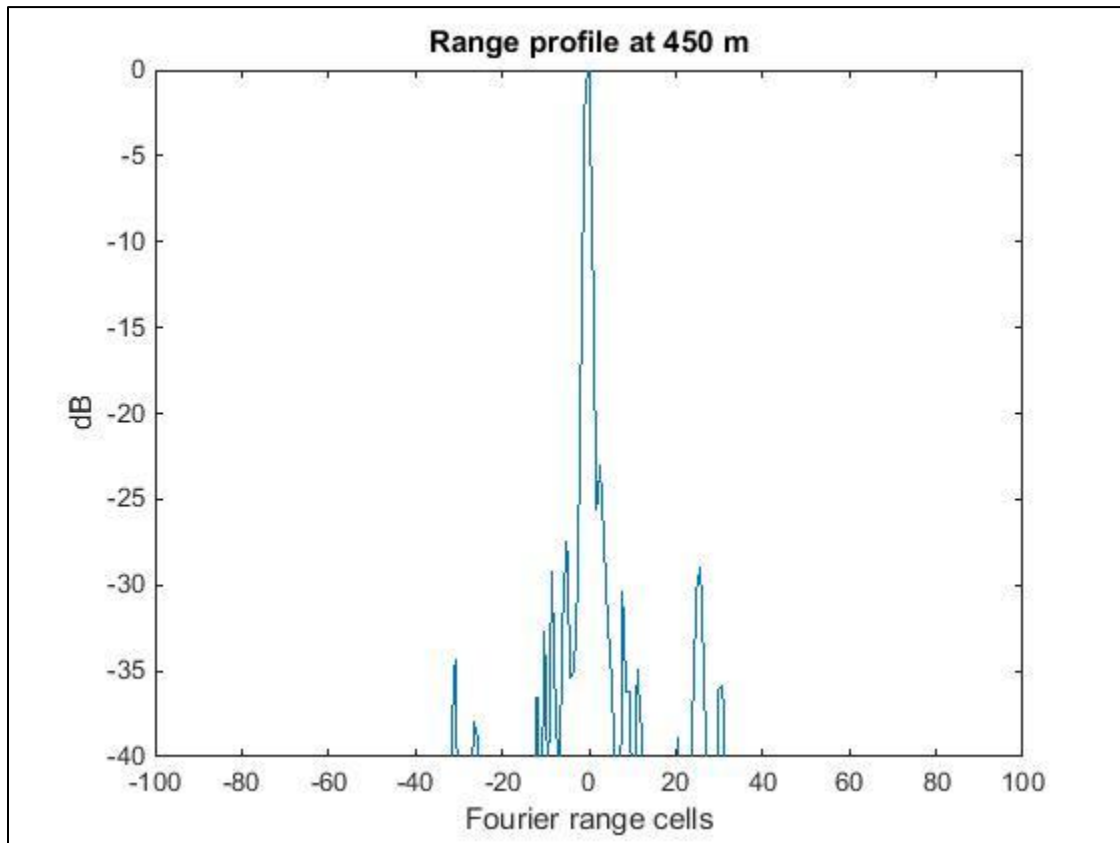


Figure 19: Range sidelobe power levels.

## 6.2. Stationary Target

The data collected from the parking garage tests were used to verify that the radar design met this requirement. Two data collection were taken at the end of the target area and as close to the radar as the target could be before it was no longer visible by the radar. The target area for this test (Figure 20) was a stretch of road that approximately matched the desired distance and range swath of the radar system.



Figure 20: Parking garage test map.

When the target was moved from the far data collect point to the near point, it was possible to view the frequency peak corresponding to the corner reflector change, shifting to a lower value. The center frequency of the SDR was set to 13 MHz. Because the final filter used before the SDR has a range of 9-19 MHz, the mixed signal processed by the laptop had values ranging from -4 to 6 MHz. As stated before, a decimation rate of 16 was used to allow the laptop to be able to store the signal.

The resulting band that the SDR could output to the laptop had a frequency range of -3.125 to 3.125 MHz. If the full bandwidth usable by the laptop was covered, the radar system's effective range for this test could be calculated as shown below:

$$\text{Minimum Distance: } \left(\frac{1}{2}\right) * (13\text{MHz} - 3.125\text{MHz}) * \left(\frac{157.9\text{us}}{1100\text{MHz}}\right) * 3e8 \text{ m/s} = 212.627\text{m} = 697.595\text{ft}$$

$$\text{Maximum Distance: } \left(\frac{1}{2}\right) * (13\text{MHz} + 3.125\text{MHz}) * \left(\frac{157.9\text{us}}{1100\text{MHz}}\right) * 3e8 \text{ m/s} = 347.201\text{m} = 1139.111\text{ft}$$

The Matlab generated FFT graphs of the two data collections show the difference in frequency values between the two points (Figure 21 and Figure 22). The frequency values were converted to distance using the same formula to calculate the minimum and maximum distance values.

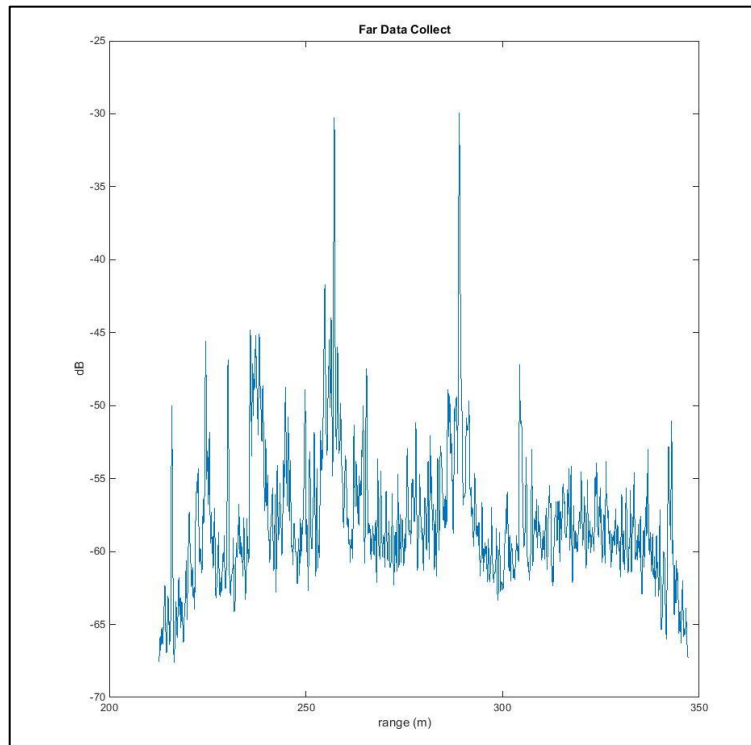


Figure 21: Far data point.

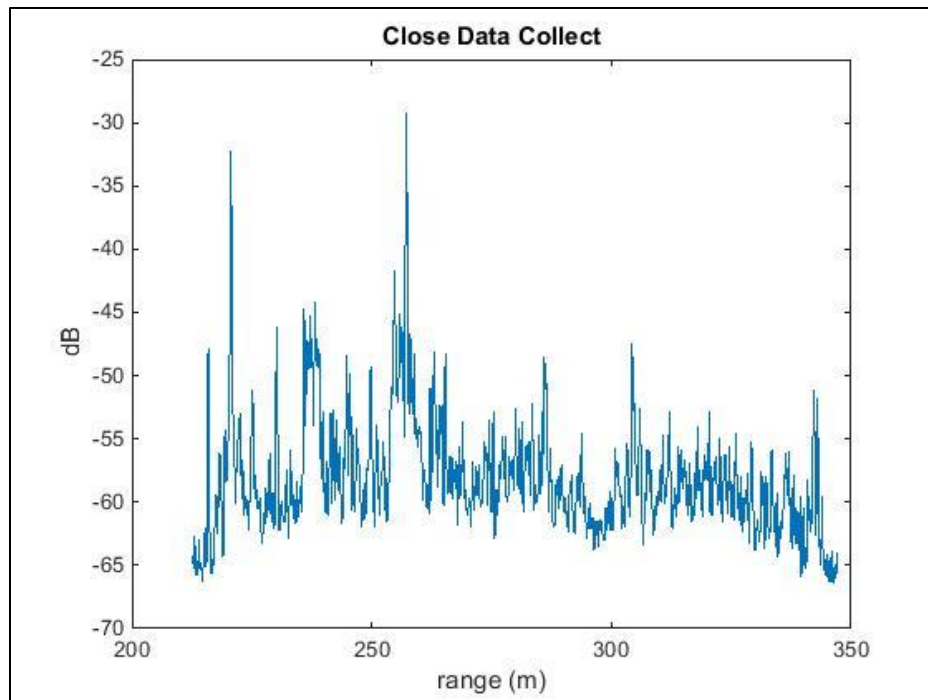


Figure 22: Close data point.

The peak of the close point corresponded to a distance of 220.6 m and a frequency of 10.244 MHz, while the far point had a distance of 289 m and a frequency of 13.419 MHz. The difference in distance to the radar between the two points is 224.41 ft. Considering that the full bandwidth that the laptop can measure was not used and that the decimation factor limited the bandwidth that could be used by the laptop to 6.25 MHz instead of the 10 MHz that the filter in the system allows, the radar design exceeds the desired range swath value of 200 ft. If a faster laptop was used to collect data, allowing the decimation value to be lowered to 8, it would be possible to use the full 10 MHz of bandwidth of the filter. The corresponding minimum and maximum detectable distances can be calculated based off of the pulse width and the cutoff frequencies of the filter.

$$\text{Minimum Distance: } \left(\frac{1}{2}\right) * (9\text{MHz}) * \left(\frac{157.9\mu\text{s}}{1100\text{MHz}}\right) * 3e8 \text{ m/s} = 193.786\text{m} = 635.781\text{ft}$$

$$\text{Maximum Distance: } \left(\frac{1}{2}\right) * (19\text{MHz}) * \left(\frac{157.9\mu\text{s}}{1100\text{MHz}}\right) * 3e8 \text{ m/s} = 409.105\text{m} = 1342.208\text{ft}$$

At a range of 707 ft, the pulse width used for this test does not support a range swath of 200 ft, as the minimum distance would need to be 607 ft. By shortening the pulse width, it would be possible to lower the minimum distance value that the radar can detect. As stated earlier, the pulse width was lengthened from the calculated 112.82us pulse width for testing purposes.

Both graphs have a high magnitude frequency peak that is not from the corner reflector at the same distance. This peak is likely due to the building next to the road where the data was collected. Prior to this project, when data was collected with the existing radar system in the same are, a high magnitude stationary target was identified at the same distance, increasing the probability that the building is the cause of the peak. The Figure 23 shows a Range-Doppler map of the target area taken over the summer. There is a high intensity target with a radial velocity of 0 (stationary) at a similar distance measured from the data collected during this project.

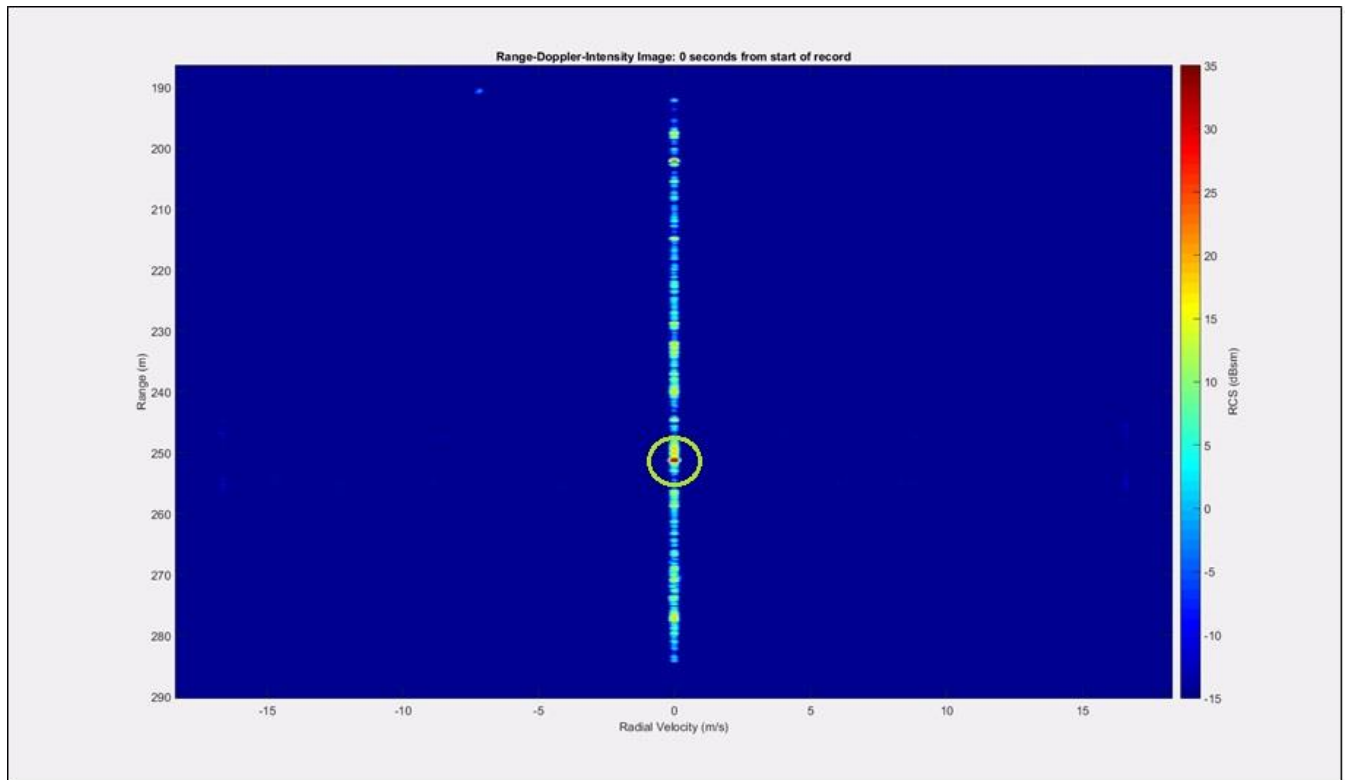


Figure 23: Data from Christopher Panuski's presentation on LiTE SAR ground data collection.

### 6.3. Moving Target

After the stationary data sets had been collected, the corner reflector was attached to a car and driven through the scene. The data was used to create a Ranged-Doppler maps to track the target moving through the scene, as shown in Figure 24. The stationary target that was seen during the stationary tests is visible as well.

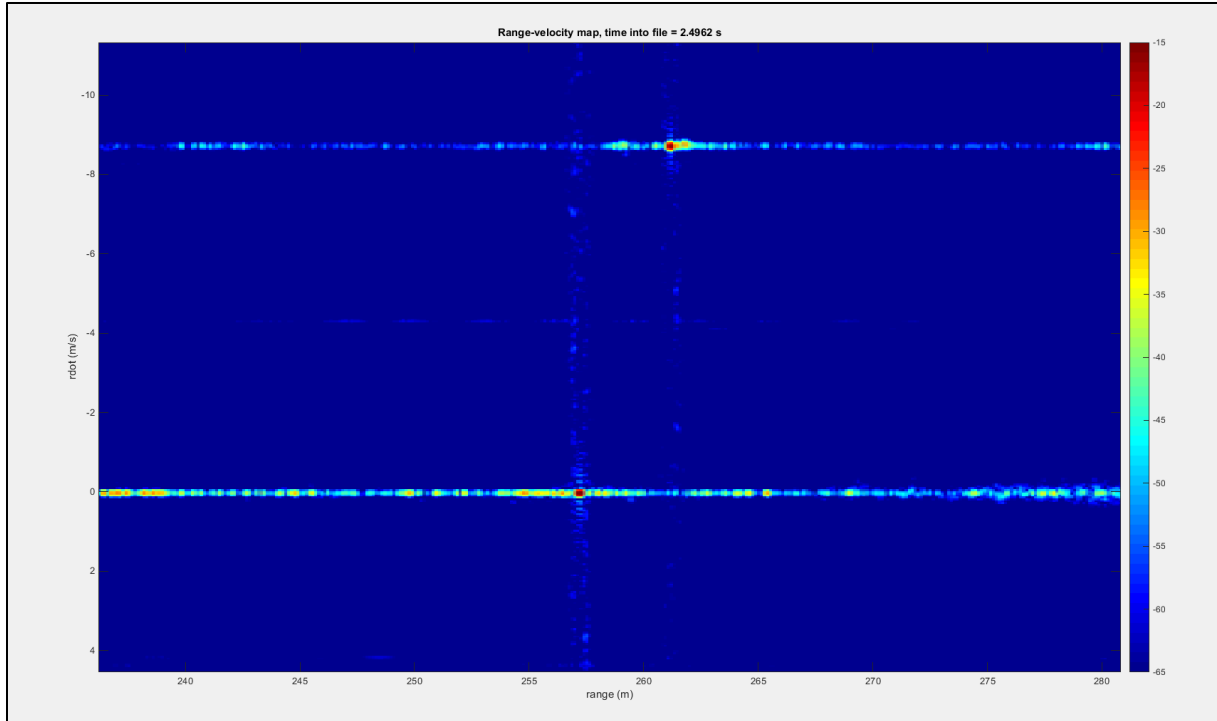


Figure 24: Ranged-Doppler graph.

While the target does have range sidelobes that span across the graph, they are about 30dB below the peak of the corner reflector's dB level. These measurements seem to match up with the range profile that was measured in the lab. When the target is zoomed into, the intensity of the response recorded by the radar system matches up with the ranged profile as well. As seen in Figure 25, both graphs have peak values at roughly the same distances apart, verifying that the measurements taken in the lab match up to real data collected from a moving target.

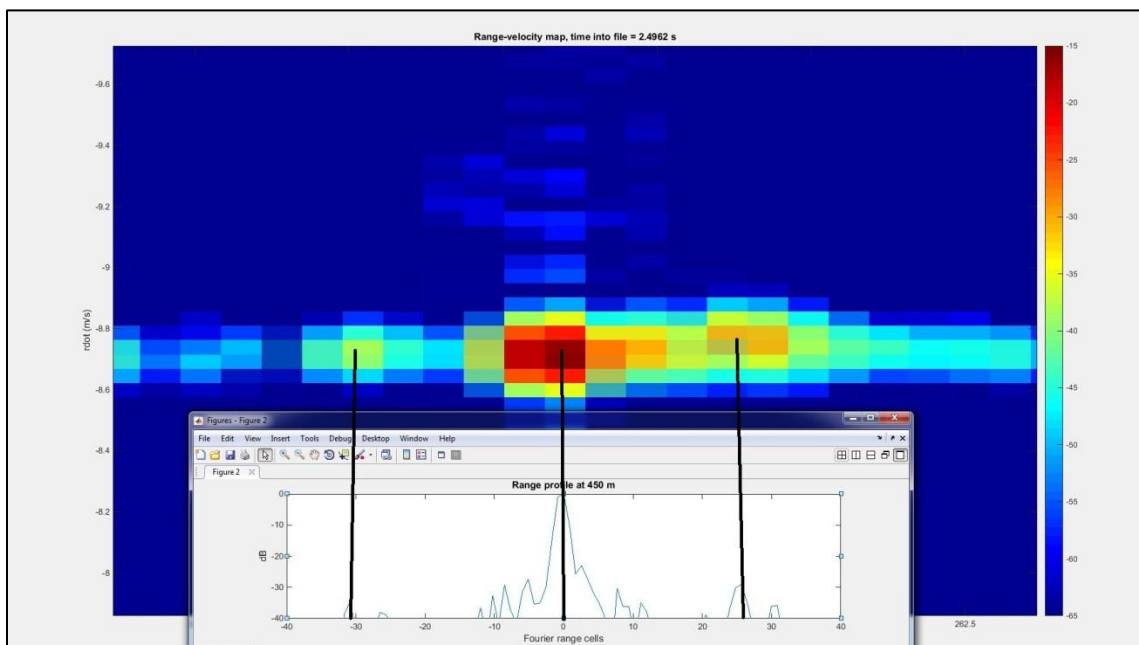


Figure 25: Ranged-Doppler compared to range profile.

One issue was found during the moving target test. As the target moves through the scene, two low  $dB$  targets move through the scene as well. When viewing the Ranged-Doppler graphs created over time, the two targets move at a constant rate and stay in line with the corner reflector and the high intensity stationary object, seen in Figure 26. Because the targets for a straight line with the corner reflector and the stationary object, the two unknown objects were determined to be intermodulated products of the corner reflector and the stationary target. The four objects also all seem to be separated by the same distance, as they would if the unknown objects were in fact intermodulation products of two known targets. A second data collection was taken of the target being driven and the two unknown objects appeared in again with the same behavior.

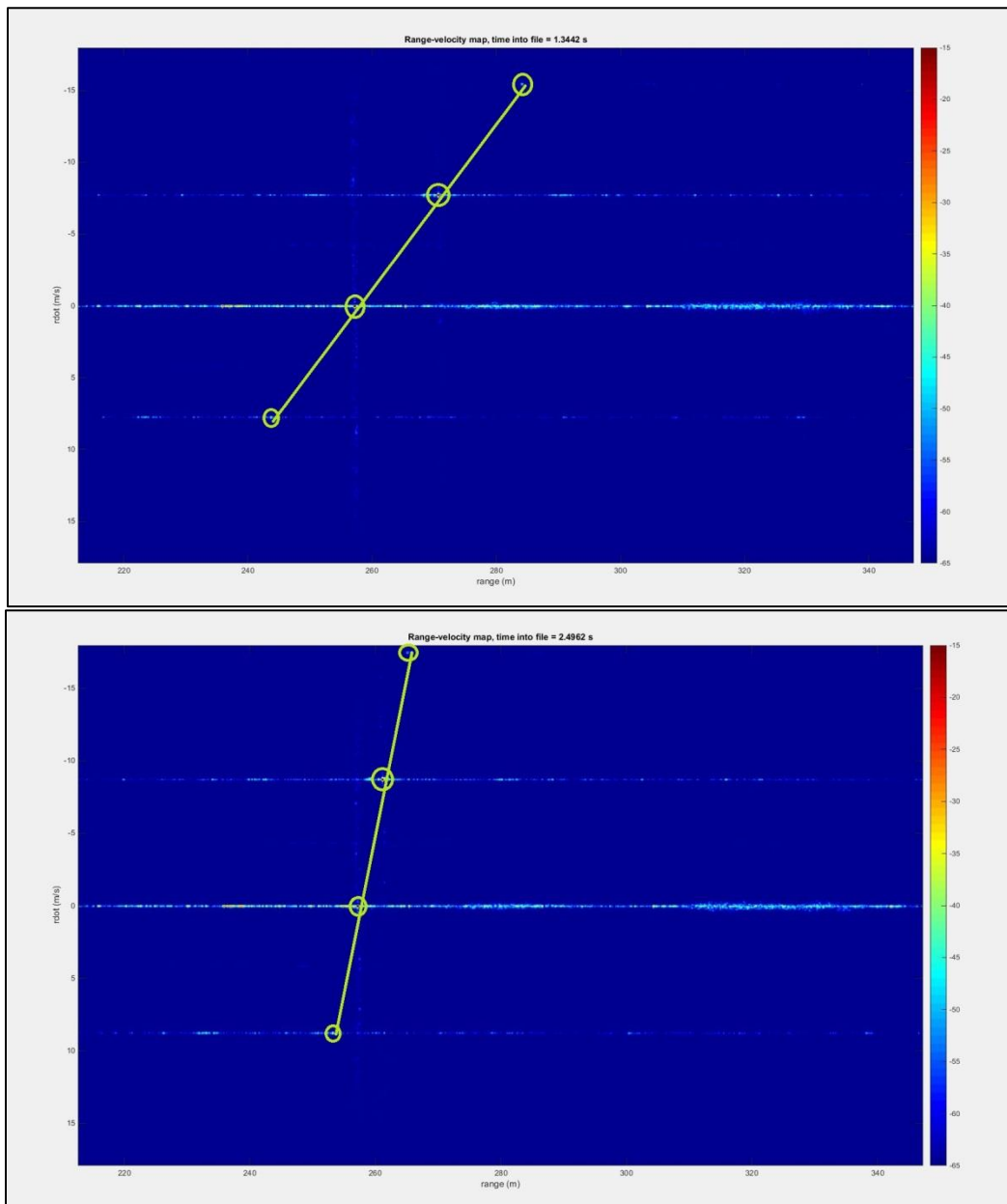


Figure 26: Extra targets in the scene.

While the two unknown targets' received signals are over 20dB below the corner reflector's signal, it was still an unexpected result that needed to be looked into. The radar was taken into the lab to be measured again. It was quickly discovered that the H626 variable gain amplifier was not producing the gain that it should. Instead of the 8-40dB gain that the specification sheet for the part claimed, the amplifier was attenuating the signal by 25dB at the lowest setting and amplifying by 5dB on the highest setting. The H626 was replaced with a fixed 30dB amplifier, as the lab did not have another variable gain amplifier that would work for this application readily available.

The radar system was tested again but with the new amplifier as well as with some new cables. It was determined that a few of the cables were damaged and affecting the performance of the radar system. When the data was analyzed (Figure 27), the intermodulated signals that were present before were not shown in the new Ranged Doppler graph. A range sidelobe power measurement was taken from the data to see if it had improved with the change in parts (Figure 28). The data set was scaled using a 40dB Taylor sidelobe control. The new range sidelobe plot showed power levels of -35dB below the peak, 10dB lower than the previous lab measurement.

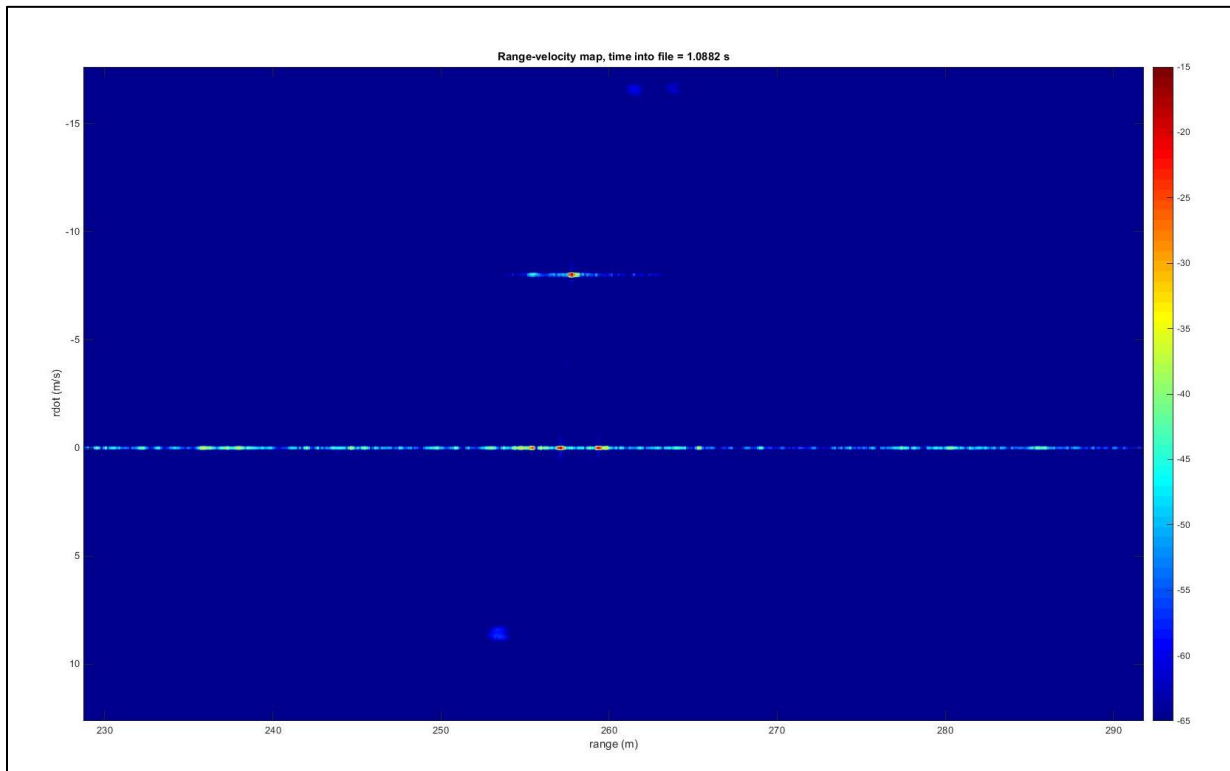


Figure 27: Intermodulation products removed.

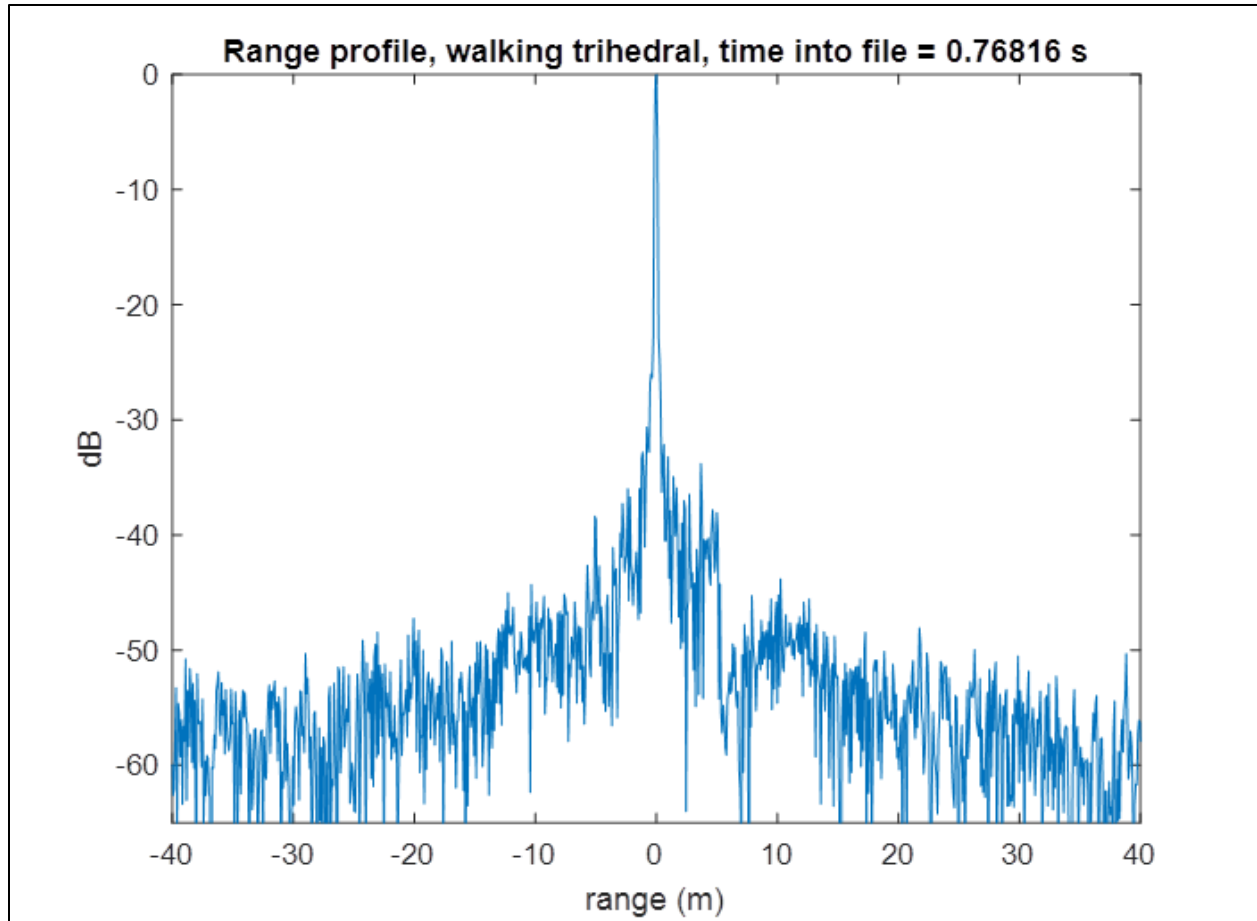


Figure 28: Updated ranged profile.

## 6.4. Calculated Results

Since the radar system could not be tested on an aircraft during the time of this project, the SAR resolution and sensitivity (Noise Equivalent Sigma Nought) had to be calculated. The formula and calculation of the SAR resolution for the system designed in this project are as follows:

$$\text{SAR Resolution: } \frac{c}{2B} = \frac{3e8}{2(1.1e9)} = 0.136\text{m} = 0.447\text{ft}$$

The desired resolution for this project's radar system was at least 1 ft. Because of the improved waveform linearity from using a digital arbitrary waveform generator, it was possible to use the entire bandwidth of the chirp that was produced. As mentioned before, the analog PLL generator used before had linearity issues at the beginning and end of the chirp that resulting in having to use less of the bandwidth of the signal in post processing. Because of this, the resolution of the existing SAR system was decreased.

To calculate the SAR sensitivity of the system designed during this project, a Matlab script created by Sandia National Laboratories was used. The equation to calculate the  $NE\sigma_0$  value used in the background is for stationary radar systems. To calculate the  $NE\sigma_0$  for a SAR system, the velocity of

aircraft and number of pulses must be accounted for as well. The script from Sandia has been used within Group 105 to calculate  $NE\sigma_0$  values in other projects, and it was recommended it be used for this project as well. The input parameters for the script are shown in Table 5. Because the antennas used for the project have Azimuth Angles of 30 degrees and the incidence angle of the antennas on an aircraft would be 45 degrees, the grazing angles to calculate the SAR sensitivity were set to 30 to 60 degrees. For a given height, differing grazing angles will give different SAR sensitivity values because the transmit and receive distances are greater for higher grazing angle values. The resulting array of  $NE\sigma_0$  were graphed and shown in Figure 29. The velocity was set to 40 m/s based off of the speed of a predator drone.

Parameter	Value
Speed of Light	299720000 m/s
Center Frequency	16.75 GHz
Wavelength	0.0179 m
Gain of Antennas	$10^{1.5}$
Altitude	$500 * 0.3048$ m
Velocity	40 m/s
Assumed Losses	5 dB
Bandwidth	1.1 GHz
Grazing Angles	30-60 degrees

Table 5: Noise equivalent sigma nought parameters.

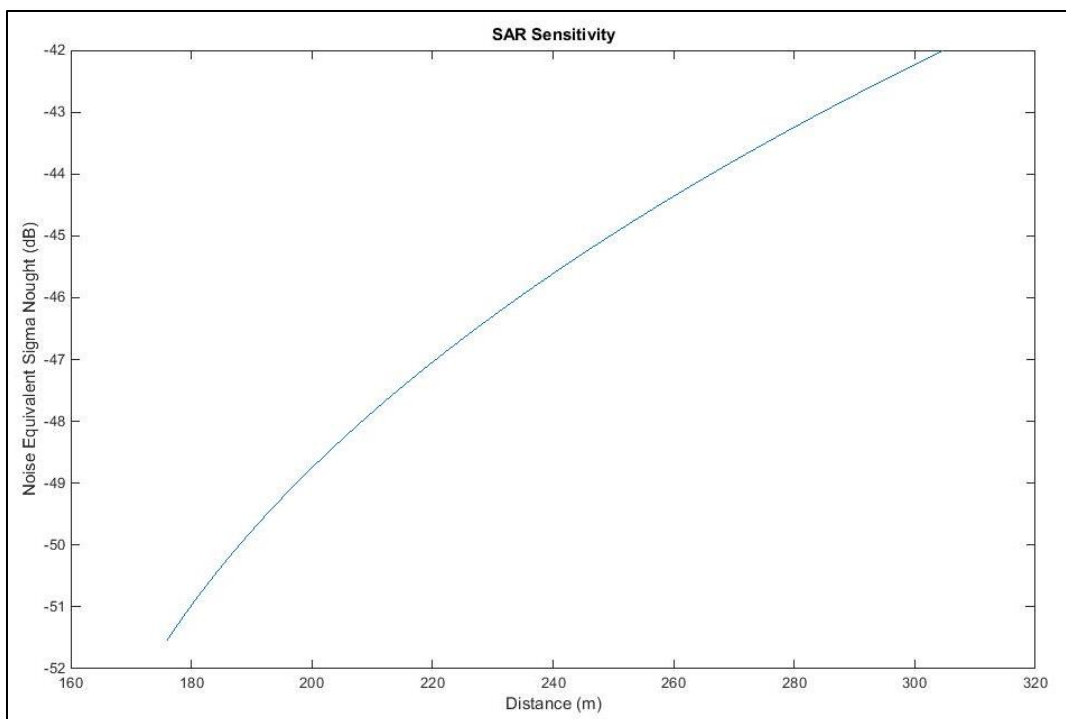


Figure 29: SAR sensitivity values.

For all distances within the range swath of the target at an altitude of 500 ft (152.4 m), the SAR sensitivity value of the radar is under the required -40dB. This should be verified by taking SAR imaging data with the system on an aircraft, but that was outside of the scope for this project.

## 7. Conclusions

Based on the requirements set for this project, the radar design and this project were successful. The radar system was able to operate in the correct frequency range and use almost all of the 1.1 GHz bandwidth. Data from testing at the parking garage showed that the radar was able to operate at the correct range with a distance swath over 200ft, so long as the correct pulse width is used. Based on measurements taken from the field test, the new radar design had lower sidelobe power levels than the initial requirements specified. When the parameters for the radar used to calculate the SAR resolution and sensitivity of the radar, the new radar design again showed that it would perform better than what was asked from by Group 105. There were however some lingering issues that were discovered during the project that were covered during the projects duration.

One of the issues found involved the laptop that was used to collect data from the SDR inside the radar. Because the laptop only had a dual core processor and 4GB of RAM, the decimation value of the data being collected by it had to be 16. While the radar system was able to collect over a minute of data without dropping any samples, with the decimation rate at 16, only 6.5 MHz of bandwidth could be used, instead of the full 10 MHz that the filter on the radar system allows. It also was not possible to perform long collections and display the data being collected in real time, because of the time required to compute an FFT on enough data to get a meaningful graph. For future collections, a different laptop should be used. Preferably, the laptop would have an Intel i7 or comparable processor and 8 or more GB of RAM. This should allow the decimation rate to be decreased to 8, or real time display of data for long collects, or both.

Even with the replaced amplifier and cables, the radar system still had unwanted signals detected and displayed in the Ranged Doppler graphs (see Figure 30). There are unwanted low power signals spanning the entire range for varying  $\dot{r}$  values. It is unclear if these values are from the need for more isolators to be put in around the amplifiers and mixers or if the power levels into the final mixer need to be amplified or attenuated. There are also low power target objects that are reflections of the high power targets in the scene. These targets could have been created by the spurious nature of the AWG. As seen in Figure 31, which is a spectrogram of the signal after the PA recorded by the 60 Gsps oscilloscope in Group 105's lab space, there are low power lines that are frequency constant as well as increasing and decreasing with time. These lines are most likely caused by the digital to analog converter on the AWG and could be removed in either post processing or directly at the output of the AWG with some form of equalization.

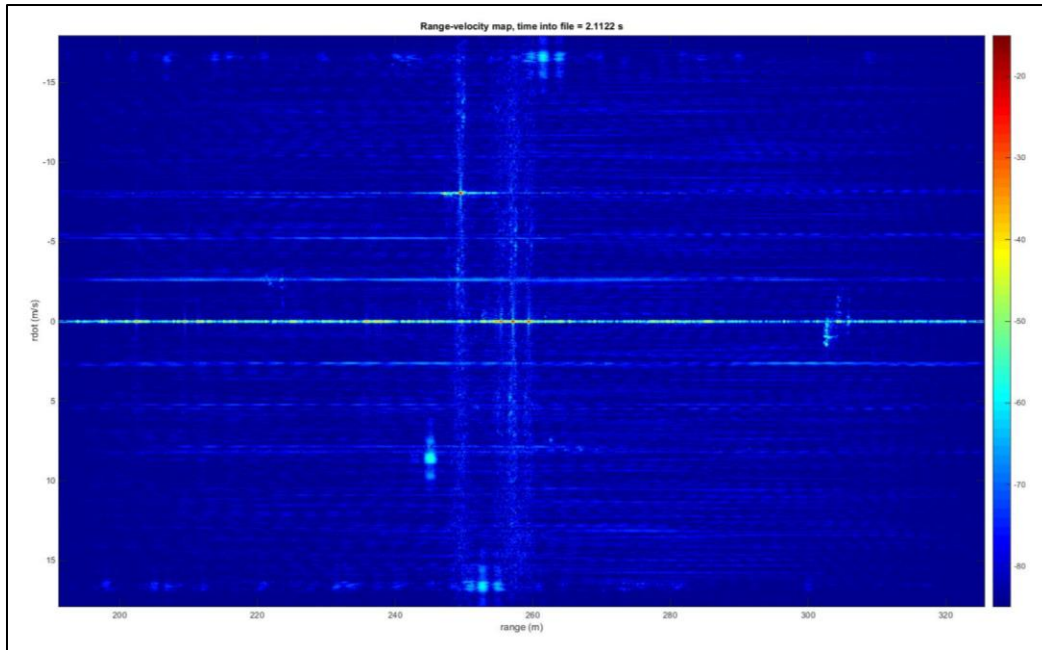


Figure 30: High dynamic range data set.

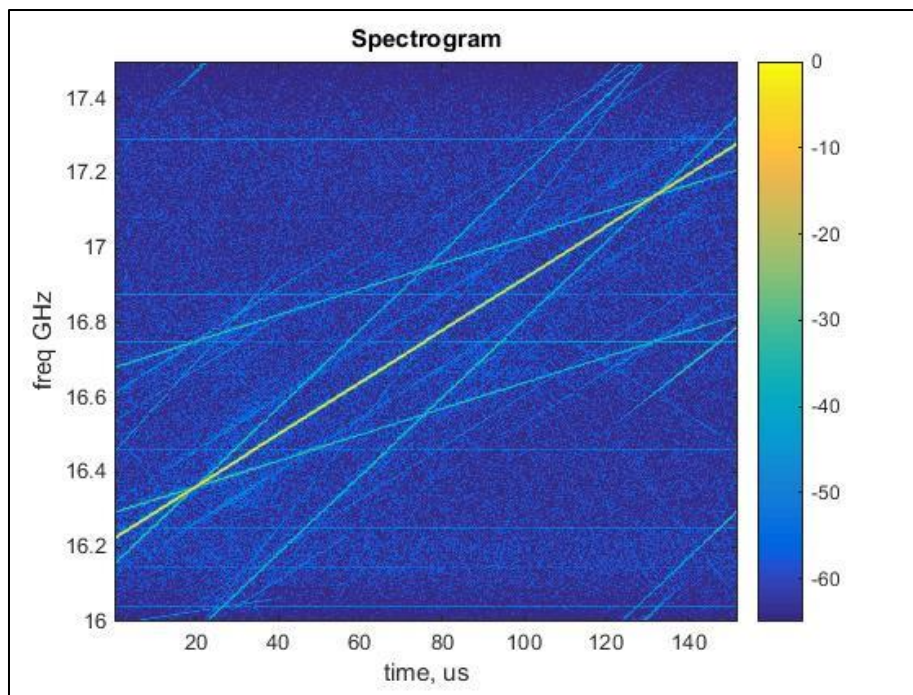


Figure 31: Spectrogram of output signal.

Even though there is still future work that needs to be done to improve the radar system designed by this project, this project can be considered a success. Group 105 now has a Ku-band instrumentation SAR, as well as system and CAD models that can be used if the radar system ever has to be rebuilt. They can also be altered to keep a record of changes made to the radar system over time by future projects.

## 8. Acknowledgements

There are many people that contributed to the success of this project that need to be acknowledged. Most of all is the project supervisor Andy Messier who helped in every aspect of the project. After Andy, there were many people who helped in many different aspects of the project, such as initial learning and setup, hardware debugging, field testing, and Matlab analysis. Jeffery Blanco and Tasadduq Hussain were instrumental in the initial learning and setup phase of the project. They helped in understanding the basics of SAR processing and getting setup in the lab for the beginning component tests. During the project, a BJT on the SDR had gone bad. When the SDR would no longer turn its LEDs on, Ricky Hardy helped debug the parts on the board. Once the bad part was identified, it was discovered that it belonged to the power protection portion of the circuit and could be bypassed. Without help from Ricky, this problem might not have been solved in time to complete the project. After the radar system had been built, Will Bartlett and Dennis Blejer helped perform the field tests. They held, walked, and drove the corner reflector through the target area, as well as helping setup the test and debug issues that arose. When all of the data was collected, it needed to be analyzed with Matlab. The functions used to process and analyze the data either belonged or were modified to fit the project by Gerald Benitz. Without his help, it would not have been possible to analyze all of the data that had been collected during this project's timeline. All of these people contributed to the success of this project and have my complete gratitude.

## 9. Bibliography

- [1] Skolnik, M. L. (1981). *Introduction to Radar Systems* F. J. Cerra (Ed.) (pp. 570). Retrieved from <https://www.google.com/url?sa=t&rct=j&q=&esrc=s&source=web&cd=1&ved=0CB4QFjAAahUKEwjw367cuufHAhXMPj4KHVJWBvM&url=https%3A%2F%2Fmaapllibrary.files.wordpress.com%2F2014%2F05%2Fintroductiontoradarsystemssecondedition-120919014912-phpapp01-1.pdf&usq=AFQjCNHWkb0o9cIR2BOPMv0IQbDXxWvJwg&bvm=bv.102022582,d.cWw&cad=rja>
- [2] Sandia National Laboratories (2014). What is Synthetic Aperture Radar (SAR)? Retrieved from [http://www.sandia.gov/radar/what\\_is\\_sar/index.html](http://www.sandia.gov/radar/what_is_sar/index.html)
- [3] Mahafza, B. R. (2013). *Radar Systems Analysis and Design Using Matlab* (Third ed.). Boca Raton, FL: CRC Press: Taylor & Francis Group.
- [4] Calabrese, D., & Episcopo, R. (2014). *Derivation of the SAR Noise Equivalent Sigma Nought*. Paper presented at the 10th European Conference on Synthetic Aperture Radar, Berlin, Germany. <http://ieeexplore.ieee.org/stamp/stamp.jsp?arnumber=6856807>
- [5] Ulaby, Moore, & Fung. (1986). Synthetic Aperture Radar. Retrieved from <http://www.csr.utexas.edu/projects/rs/whatisar/sar.html>
- [6] Yarman, E., Yazici, B., & Cheney, M. (2008). Bistatic Synthetic Aperture Radar Imaging for Arbitrary Flight Trajectories. *IEEE Transactions on Image Processing*, 17(1), 84-93. Retrieved from IEEE Xplore Digital Library website: <http://ieeexplore.ieee.org/stamp/stamp.jsp?arnumber=4392497>
- [7] Gierull, C. (2004). *Bistatic Synthetic Aperture Radar: TIF - Report (Phase 1)*. University of British Columbia Retrieved from <http://www.ece.ubc.ca/~yewn/papers/DRDCbistatic.pdf>.